The protonmotive force and respiratory control:

Building blocks of mitochondrial physiology

Part 1.

MitoEAGLE Network

Corresponding author: Gnaiger E

Contributing co-authors

Ahn B, Alves MG, Beard DA, Ben-Shachar D, Bishop D, Breton S, Brown GC, Brown RA, Buettner GR, Cervinkova Z, Chicco AJ, Coen PM, Collins JL, Crisóstomo L, Davis MS, Dias T, Distefano G, Doerrier C, Ehinger J, Elmer E, Fell DA, Filipovska A, Fisher J, Garcia-Roves PM, Garcia-Souza LF, Genova ML, Gonzalo H, Goodpaster BH, Han J, Harrison DK, Hellgren KT, Hernansanz P, Holland O, Hoppel CL, Iglesias-Gonzalez J, Irving BA, Iyer S, Jansen-Dürr P, Jespersen NR, Jha RK, Käämbre T, Kane DA, Kappler L, Keijer J, Komlodi T, Krako Jakovljevic N, Kuang J, Labieniec-Watala M, Laner V, Lee HK, Lemieux H, Lerfall J, Lucchinetti E, Makrecka-Kuka M, Meszaros AT, Moisoi N, Molina AJA, Montaigne D, Moore AL, Murray AJ, Newsom S, Nozickova K, Oliveira PF, Oliveira PJ, Orynbayeva Z, Palmeira CM, Patel HH, Pesta D, Petit PX, Pichaud N, Pirkmajer S, Porter RK, Pranger F, Prochownik EV, Reboredo P, Renner-Sattler K, Robinson MM, Rohlena J, Røsland GV, Rossiter HB, Salvadego D, Scatena R, Schartner M, Scheibye-Knudsen M, Schilling JM, Schlattner U, Schoenfeld P, Scott GR, Singer D, Sobotka O, Spinazzi M, Stocker R, Sumbalova Z, Suravajhala P, Tanaka M, Tandler B, Tepp K, Towheed A, Trivigno C, Tronstad KJ, Tyrrell DJ, Velika B, Vendelin M, Vercesi AE, Ward ML, Watala C, Wei YH, Wieckowski MR, Wolff J, Wuest RCI, Zaugg M, Zorzano A

27

28 Supporting co-authors:

29 Arandarčikaitė O, Åsander Frostner E, Bakker BM, Batista Ferreira J, Bernardi P, Boetker

30 HE, Borsheim E, Borutaitė V, Bouitbir J, Calabria E, Calbet JA, Carvalho E, Chaurasia B,

31 Clementi E, Collin A, Das AM, De Palma C, Dubouchaud H, Duchen MR, Durham WJ,

32 Dyrstad SE, Fornaro M, Gan Z, Garlid KD, Garten A, Gourlay CW, Granata C, Haas CB,

33 Haendeler J, Hand SC, Hepple RT, Hickey AJ, Hoel F, Kainulainen H, Keppner G, Khamoui

34 AV, Klingenspor M, Koopman WJH, Kowaltowski AJ, Krajcova A, Lenaz G, MacMillan-

35 Crow LA, Malik A, Markova M, Mazat JP, Menze MA, Methner A, Muntané J, Muntean

36 DM, Neuzil J, O'Gorman D, Oliveira MT, Pak YMK, Pettersen IKN, Pulinilkunnil T, Ropelle

37 ER, Salin K, Sandi C, Sazanov LA, Siewiera K, Silber AM, Skolik R, Smenes BT, Soares

38 FAA, Sokolova I, Sonkar VK, Stankova P, Swerdlow RH, Szabo I, Thyfault JP, Tretter L,

39 Vieyra A, Votion DM, Williams C, Zaugg K

40

41 **Updates:**

42

43

Correspondence: Gnaiger E

Department of Visceral, Transplant and Thoracic Surgery, D. Swarovski Research Laboratory, Medical University of Innsbruck, Innrain 66/4, A-6020 Innsbruck, Austria

Email: erich.gnaiger@i-med.ac.at

Tel: +43 512 566796, Fax: +43 512 566796 20

*This manuscript on 'The protonmotive force and respiratory control' is a position statement in the frame of COST Action CA15203 MitoEAGLE. The list of co-authors evolved from MitoEAGLE Working Group Meetings and a **bottom-up** spirit of COST in phase 1: This is an open invitation to scientists and students to join as co-authors, to provide a balanced view on mitochondrial respiratory control, a fundamental introductory presentation of the concept of the protonmotive force, and a consensus statement on reporting data of mitochondrial respiration in terms of metabolic flows and fluxes. We plan a series of follow-up reports by the expanding MitoEAGLE Network, to increase the scope of recommendations on harmonization and facilitate global communication and collaboration.*
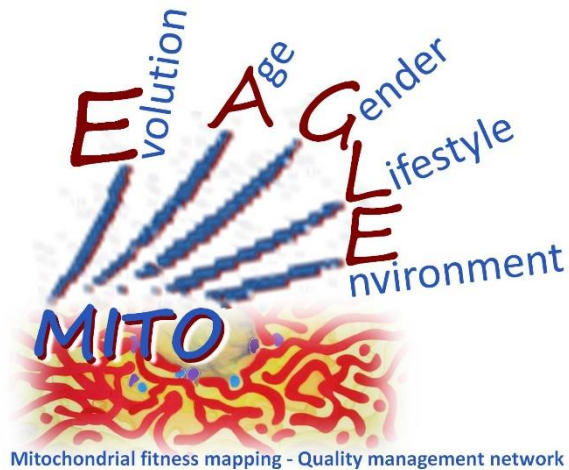
*Phase 2 - until **October 12:** We continue to invite comments and suggestions on the MitoEAGLE preprint, particularly if you are an **early career investigator adding an open future-oriented perspective**, or an **established scientist providing a balanced historical basis**. Your critical input into the quality of the manuscript will be most welcome, improving our aims to be educational, general, consensus-oriented, and practically helpful for students working in mitochondrial respiratory physiology.*

To join as a co-author, please feel free to focus on a particular section in terms of direct input and references, contributing to the scope of the manuscript from the perspective of your expertise. Your comments will be largely posted on the discussion page of the MitoEAGLE preprint website.

If you prefer to submit comments in the format of a referee's evaluation rather than a contribution as a co-author, I will be glad to distribute your views to the updated list of co-authors for a balanced response. We would ask for your consent on this open bottom-up policy.

We organize a MitoEAGLE session linked to our series of reports at the MiPconference Nov 2017 in Hradec Kralove in close association with the MiPsociety (where you hopefully will attend) and at EBEC 2018 in Budapest.

» http://www.mitoeagle.org/index.php/MiP2017_Hradec_Kralove_CZ

I thank you in advance for your feedback.
With best wishes,

Erich Gnaiger
Chair Mitochondrial Physiology Society - http://www.mitophysiology.org
Chair COST Action MitoEAGLE - http://www.mitoeagle.org
Medical University of Innsbruck, Austria

Contents

140 **Abstract**

141 Clarity of concepts and consistency of nomenclature are trademarks of a research field across

142 its specializations, facilitating transdisciplinary communication and education. As research and

143 knowledge of mitochondrial physiology expand, the necessity for harmonizing nomenclature

144 concerning mitochondrial respiratory states and rates has become apparent. Peter Mitchell's

145 concept of the protonmotive force establishes the links between electrical and chemical

146 components of energy transformation and coupling in oxidative phosphorylation. This unifying

147 concept provides the framework for developing a consistent terminology of mitochondrial

148 physiology and bioenergetics. We follow IUPAC guidelines on general terms of physical

149 chemistry, extended by concepts of open systems and irreversible thermodynamics. We align

150 the nomenclature of classical bioenergetics on respiratory states with a concept-driven

151 constructive terminology to address the meaning of each respiratory state. Standards for

152 evaluation of respiratory states must be followed for the development of databases of

153 mitochondrial respiratory function in species, tissues and cells studied under diverse

154 physiological and experimental conditions.

155

160

161

Box 1:

In brief: mitochondria and Bioblasts

> * Does the public expect biologists to understand Darwin's theory of evolution?
> * Do students expect that researchers of bioenergetics can explain Mitchell's theory of chemiosmotic energy transformation?

Mitochondria are dynamic organelles contained within eukaryotic cells, with a double membrane. The inner mitochondrial membrane shows dynamic tubular and disk-shaped cristae that separate the mitochondrial matrix, *i.e.* the internal mitochondrial compartment, and the intermembrane space; the latter being enclosed by the outer mitochondrial membrane. Mitochondria were described for the first time in 1857 by Rudolph Albert von Kölliker as granular structures or 'sarkosomes'. In 1886 Richard Altman called them 'bioblasts' (published 1894). The word 'mitochondrium' (Greek mitos: thread; chondros: granule) was introduced by Carl Benda (1898). Mitochondria are the oxygen consuming electrochemical generators which evolved from endosymbiotic bacteria (Margulis 1970). The bioblasts of Richard Altmann (1894) include not only the mitochondria as presently defined, but also symbiotic and free-living bacteria. Mitochondria are the structural and functional elemental units of cell respiration, where cell respiration is defined as the consumption of oxygen coupled to electrochemical proton translocation across the inner mitochondrial membrane. In the process of oxidative phosphorylation (OXPHOS), the reduction of O_2 is electrochemically coupled to conservation of energy in the form of ATP (Mitchell 2011). As part of the OXPHOS system, these powerhouses of the cell contain the transmembrane respiratory complexes (i.e. FMN, Fe-S and cytochrome *b*, *c*, aa_3 redox systems), alternative dehydrogenases and oxidases, the coenzyme ubiquinone (coenzyme Q) and ATP synthase together with the enzymes of the tricarboxylic acid cycle and the fatty acid oxidation enzymes, ion transporters, including substrate, co-factor and metabolite transporters as well as proton pumps, and mitochondrial kinases related to energy transfer pathways. The mitochondrial proteome comprises over 1,200 proteins (Mitocharta), mostly encoded by nuclear DNA (nDNA), with a variety of functions, many of

189 which are relatively well known (*e.g.* apoptosis-regulating proteins), are still under

190 investigation, or need to be identified (alanine transporter). Mitochondria maintain several

191 copies of their own genome (hundred to thousands per cell) which is maternally inherited and

192 known as mitochondrial DNA (mtDNA). mtDNA is 16.5 Kb in length, contains 13 protein-

193 coding genes for subunits of the transmembrane respiratory Complexes CI, CIII, CIV and ATP

194 synthase, and also encodes 22 tRNAs and the mitochondrial 16S and 12S rRNA. The

195 mitochondrial genome is both regulated and supplemented by nuclear-encoded mitochondrial

196 targeted proteins. Evidence has accumulated that additional gene content is encoded in the

197 mitochondrial genome, e.g. microRNAs, smithRNAs, and even additional proteins. The inner

198 mitochondrial membrane contains the non-bilayer phospholipid cardiolipin, which is not

199 present in any other eukaryotic cellular membrane. Cardiolipin promotes the formation of

200 respiratory supercomplexes, which are supramolecular assemblies based upon specific, though

201 dynamic, interactions between individual respiratory complexes (Lenaz *et al.* 2017). There is a

202 constant crosstalk between mitochondria and the other cellular components at the

203 transcriptional or post-translational level, and through cell signalling in response to varying

204 energy demands (Quiros *et al.* 2016). Mitochondrial morphology can change in response to

205 energy requirements of the cell via processes known as fusion and fission through which

206 mitochondria can communicate within a network, and in various pathological states which

207 cause swelling or dysregulation of fission and fusion. Mitochondrial dysfunction is associated

208 with a wide variety of genetic and degenerative diseases. Therefore, a better understanding of

209 mitochondrial physiology will improve our understanding of the etiology of disease and the

210 diagnostic repertoire of mitochondrial medicine. Abbreviation: mt, as generally used in

211 mtDNA. Mitochondrion is singular and mitochondria is plural.

212   *'For the physiologist, mitochondria afforded the first opportunity for an experimental*

213 *approach to structure-function relationships, in particular those involved in active transport,*

214 *vectorial metabolism, and metabolic control mechanisms on a subcellular level'* (Ernster and

215 Schatz 1981).

216 _____

1. Introduction

218   Mitochondria are the powerhouses of the cell with numerous physiological, molecular,

219 and genetic functions (**Box 1**). Every study of mitochondrial function and disease is faced with

220 **E**volution, **A**ge, **G**ender and sex, **L**ifestyle, and **E**nvironment (EAGLE) as essential background

221 conditions characterizing the individual patient or subject, cohort, species, tissue and to some

222 extent even cell line. As a large and highly coordinated group of laboratories and researchers,

223 the global MitoEAGLE Network's mission is to generate the necessary scale, type, and quality

224 of consistent data sets and conditions to address this intrinsic complexity. Harmonization of

225 experimental protocols and implementation of a quality control and data management system

226 is required to interrelate results gathered across a spectrum of studies and to generate a

227 rigorously monitored database focused on mitochondrial respiratory function. In this way,

228 researchers within the same and across different disciplines will be positioned to compare their

229 findings to an agreed upon set of clearly defined and accepted international standards.

230   Reliability and comparability of quantitative results depend on the accuracy of

231 measurements under strictly-defined conditions. A conceptually clearly-defined framework is

232 also required to warrant meaningful interpretation and comparability of experimental outcomes

233 carried out by research groups at different institutes. With an emphasis on quality of research,

234 collected data can be useful far beyond the specific question of a specific experiment. Vague or

235 ambiguous jargon can lead to confusion and may relegate valuable signals to wasteful noise.

236 For this reason, measured values must be expressed in standardized units for each parameter

237 used to define mitochondrial respiratory function. Standardization of nomenclature and

238 technical terms is essential to improve the awareness of the intricate meaning of divergent

239 scientific vocabulary. The focus on coupling states in mitochondrial preparations is a first step

240   in the attempt to generate a harmonized and conceptually oriented nomenclature in

241   bioenergetics and mitochondrial physiology. Coupling states of intact cells and respiratory

242   control by fuel substrates and specific inhibitors of respiratory enzymes will be reviewed in

243   subsequent communications.

244

245   **2. Respiratory coupling states in mitochondrial preparations**

246   *'Every professional group develops its own technical jargon for talking about*

247   *matters of critical concern ... People who know a word can share that idea with*

248   *other members of their group, and a shared vocabulary is part of the glue that holds*

249   *people together and allows them to create a shared culture'* (Miller 1991).

250   *2.1. Definitions*

251   **Mitochondrial preparations** are defined as either isolated mitochondria, or tissue and

252   cellular preparations in which the barrier function of the plasma membrane is disrupted. The

253   plasma membrane separates the cytosol, nucleus and organelles (the intracellular compartment)

254   from the environment of the cell. The plasma membrane consists of a lipid bilayer, embedded

255   proteins and attached organic molecules which collectively control the selective permeability

256   of ions, organic molecules and particles across the cell boundary. The intact plasma membrane,

257   therefore, prevents the passage of many water-soluble mitochondrial substrates, such as

258   succinate or ADP, that are required for the analysis of respiratory capacity at kinetically

259   saturating concentrations, thus limiting the scope of investigations into mitochondrial

260   respiratory function in intact cells. The cholesterol content of the plasma membrane is high

261   compared to mitochondrial membranes. Therefore, mild detergents, such as digitonin and

262   saponin, can be applied to selectively permeabilize the plasma membrane by interaction with

263   cholesterol and allow free exchange of cytosolic components with ions and organic molecules

264   of the immediate cell environment, while maintaining the integrity and localization of

265   organelles, cytoskeleton and the nucleus. Application of optimum concentrations of these mild

266 detergents leads to the complete loss of cell viability, tested by nuclear staining, while

267 mitochondrial function remains unaffected, as shown by the lack of a respiratory response of

268 respiration of isolated mitochondria to the addition of such low concentrations of digitonin and

269 saponin. Mechanical or chemical permeabilization is applied in tissue homogenates containing

270 all components of the cell in the crude homogenate at highly diluted concentrations. Likewise,

271 in permeabilized tissues or cells the functional and structural integrity of mitochondria are

272 largely maintained. All mitochondria are retained in chemically permeabilized mitochondrial

273 preparations and crude tissue homogenates. In the preparation of isolated mitochondria the cells

274 or tissues are homogenized, and the mitochondria are separated from other cell fractions and

275 purified by centrifugation, entailing the loss of a significant fraction of mitochondria. The term

276 mitochondrial preparation does not include further fractionation of mitochondrial components,

277 as well as submitochondrial particles.

278 **Control and regulation:** The terms metabolic *control* and *regulation* are frequently used

279 synonymously, but are distinguished in metabolic control analysis: 'We could understand the

280 regulation as the mechanism that occurs when a system maintains some variable constant over

281 time, in spite of fluctuations in external conditions (homeostasis of the internal state). On the

282 other hand, metabolic control is the power to change the state of the metabolism in response to

283 an external signal' (Fell 1997). Respiratory control may be induced by experimental control

284 signals that *exert* an influence on: (*1*) ATP demand and ADP phosphorylation rate; (*2*) fuel

285 substrate, pathway competition and oxygen availability, *e.g.*, starvation and hypoxia; (*3*) the

286 protonmotive force, redox states, flux-force relationships, coupling and efficiency; (*4*) Ca^{2+} and

287 other ions including H^+; (*5*) inhibitors, *e.g.*, nitric oxide or intermediary metabolites, such as

288 oxaloacetate. *Mechanisms* of respiratory control and regulation include adjustments of (*1*)

289 enzyme activities by allosteric mechanisms and phosphorylation, (*2*) enzyme content,

290 concentrations of cofactors and conserved moieties (such as adenylates, nicotinamide adenine

291 dinucleotide [NAD^+/NADH], coenzyme Q, cytochrome *c*); (*3*) metabolic channeling by

292   supercomplexes; and *(4)* mitochondrial density (enzyme concentrations and membrane area)

293   and morphology (cristae folding, fission and fusion). (5) Mitochondria are targeted directly by

294   hormones, thereby affecting their energy metabolism (Lee *et al.* 2013; Gerö and Szabo 2016;

295   Price and Dai 2016; Moreno *et al.* 2017). Evolutionary or acquired differences in the genetic

296   and epigenetic basis of mitochondrial function (or dysfunction) between subjects and gene

297   therapy; age; gender, biological sex, and hormone concentrations; life style including exercise

298   and nutrition; and environmental issues including thermal, atmospheric, toxicological and

299   pharmacological factors, exert an influence on all control mechanisms listed above (for reviews,

300   see Brown 1992; Gnaiger 1993a, 2009; 2014; Paradies *et al.* 2014; Morrow *et al*. 2017).

301   **Respiratory control and response:** There is a difference between control by a fixed

302   component of a metabolic system or module, e.g. ATP synthase, and the response to an

303   experimental variable, *e.g.*, fuel substrate or ADP. Whilst lack of control by a metabolic

304   module, *e.g.* phosphorylation system, does mean that there will be no response to a variable

305   activating it, *e.g.* [ADP], the reverse is not true; *i.e.*, lack of response to [ADP] does not exclude

306   the phosphorylation system from having some degree of control. The degree of control of a

307   component of the OXPHOS system on an output variable of the system, such as oxygen flux,

308   will in general be different from the degree of control on other outputs, such as phosphorylation

309   flux, cytochrome redox states, protonmotive force, phosphorylation potential, and proton leak

310   flux (**Box 2**). As such, it is necessary to be specific as to which output is under consideration.

311   Respiratory control is insufficiently specific in the context of specific interpretations (Fell

312   1997).

313   **Respiratory coupling control:** Respiratory control is monitored in a mitochondrial

314   preparation under conditions defined as respiratory states. When phosphorylation of ADP to

315   ATP is stimulated or depressed, an increase or decrease is observed in electron flux linked to

316   oxygen consumption in 'controlled' coupling states in intact mitochondria. Alternatively,

317   coupling of electron transfer with phosphorylation is disengaged by disruption of the integrity

318 of the inner mitochondrial membrane or by uncouplers, functioning like a clutch in a

319 mechanical system. The corresponding coupling control state is characterized by high levels of

320 oxygen consumption without control by phosphorylation ('uncontrolled state'; classical

321 terminology). Energetic coupling is defined in **Box 3**. Respiratory control refers to the ability

322 of mitochondria to adjust oxygen consumption in response to external control signals by

323 engaging various mechanisms of control and regulation. Loss of coupling by intrinsic

324 uncoupling and decoupling, or pathological dyscoupling lowers the efficiency. Such

325 generalized uncoupling is different from switching to mitochondrial pathways that involve

326 fewer than three proton pumps ('coupling sites': Complexes CI, CIII and CIV), bypassing CI

327 through multiple electron entries into the Q-junction (**Fig. 1**). A bypass of CIII and CIV is

328 provided by alternative oxidases, which reduce oxygen without proton translocation.

329 Reprogramming of mitochondrial pathways may be considered as a switch of gears (changing

330 the stoichiometry) rather than uncoupling (loosening the stoichiometry).

331   **Pathway control states** are obtained in mitochondrial preparations by depletion of

332 endogenous substrates and addition to the mitochondrial respiration medium of fuel substrates

333 (CHNO) and specific inhibitors, activating selected mitochondrial pathways (**Fig. 1**). Coupling

334 control states and pathway control states are complementary, since mitochondrial preparations

335 depend on an exogenous supply of pathway-specific fuel substrates and oxygen (Gnaiger 2014).

336

---

337 **Box 2: Metabolic fluxes and flows: vectorial and scalar**

338 In the mitochondrial electron transfer system (**Fig. 1**), vectorial transmembrane proton flux is

339 coupled through the proton pumps CI, CIII and CIV to the catabolic flux of scalar reactions,

340 collectively measured as oxygen flux. In **Fig. 2**, the scalar catabolic reaction, k, of oxygen

341 consumption, $J_{O2,k}$ [mol·s^{-1}·m^{-3}], is expressed as oxygen flux per volume, V [m^3], of the

342 experimental chamber (the system). Fluxes are *vectors*, if they have *spatial* direction in addition

343 to magnitude. A vector flux (surface-density of flow) is expressed per unit cross-sectional area,

344   *A* [m^2], perpendicular to the direction of flux. If *flows, I,* are defined as extensive quantities of

345   the *system*, as vector or scalar flow, $\boldsymbol{I}$ or I [mol·s^{-1}], respectively, then the corresponding vector

346   and scalar *fluxes, J,* are obtained as $\boldsymbol{J}=\boldsymbol{I}\cdot A^{-1}$ [mol·s^{-1}·m^{-2}] and $J=I\cdot V^{-1}$ [mol·s^{-1}·m^{-3}], respectively,

347   expressing flux as an area-specific vector or volume-specific scalar quantity. Volume-specific

348   scalar O$_2$ flux is coupled (**Box 3**) to vectorial translocation of protons across the inner

349   mitochondrial membrane, from the negative compartment (matrix space; N-phase) to the

350   positive compartment (inter-membrane space; P-phase; **Fig. 2**). The *scalar or compartmental*

351   direction of a chemical reaction, A → B, is defined by assigning substrates and products, A and

352   B, as energetic 'compartments' (O$_2$ is defined as a substrate in respiratory O$_2$ consumption). In

353   direct analogy to A → B, the compartmental direction of a vectorial translocation (*e.g.*

354   diffusion) from the N-phase to the P-phase is defined by assigning the initial and final state as

355   energetic compartments, H$^+_{in}$ → H$^+_{out}$, respectively (Gnaiger 1993b). Vectorial transmembrane

356   proton flux, $J_{H+,out}$, is analyzed in a heterogenous compartmental system as a quantity with

357   *directional* but not *spacial* information. In order to establish a quantitative relation between the

358   coupled fluxes, both $J_{O2,k}$ and $J_{H+,out}$ must be expressed in identical units ([mol·s^{-1}·m^{-3}] or

359   [C·s^{-1}·m^{-3}]), yielding the H$^+_{out}$/O$_2$ ratio (**Fig. 1**). The *vectorial* proton flux in compartmental

360   translocation has *compartmental direction*, distinguished from a *vector* flux with *spatial*

361   *direction*. Likewise, the corresponding protonmotive force is defined as an electrochemical

362   potential *difference* between two compartments, which is different from a vector force or

363   *gradient* across the membrane with defined spatial direction.

364

365   *2.2. Three coupling states of mitochondrial preparations and residual oxygen consumption*

366   **Coupling control states:** To extend the classical nomenclature on mitochondrial

367   coupling states (Section 2.3) by a concept-driven terminology that incorporates explicit

368   information on the nature of the respiratory states, the terminology must be general and not

369   restricted to any particular experimental protocol or mitochondrial preparation (Gnaiger 2009).

370   We focus primarily on the conceptual 'why', along with clarification of the experimental 'how'.

371   In the following section, the concept-driven terminology is explained and coupling states are

372   defined. The capacity of *oxidative phosphorylation*, OXPHOS, provides diagnostic reference

373   values for physiological respiratory capacities of defined pathways of core energy metabolism

374   and is, therefore, measured at kinetically saturating concentrations of ADP and inorganic

375   phosphate, P_i. The *oxidative* capacity of the electron transfer system, ETS, reveals the limitation

376   of OXPHOS capacity mediated by the *phosphorylation* system. ETS capacity is measured as

377   noncoupled respiration by application of *external uncouplers*. The contribution of *intrinsically*

378   *uncoupled* oxygen consumption is most easily studied by not stimulating or arresting

379   phosphorylation, when oxygen consumption compensates mainly for the proton leak; the

380   corresponding states are collectively classified as LEAK states (**Table 1**). Coupling states of

381   mitochondrial preparations can be compared in any defined mitochondrial pathway control state

382   (**Fig. 1**). Fuel substrates and ETS inhibitors are kept constant while (*1*) adding ADP or P_i, (*2*)

383   inhibiting the phosphorylation system, and (*3*) performing uncoupler titrations.

384   **Respiratory capacities and kinetic control:** Coupling control states are established in

385   the study of mitochondrial preparations to obtain reference values for various output variables.

386   Physiological conditions *in vivo* may deviate substantially from these experimentally obtained

387   states. Since kinetically saturating concentrations, *e.g.* of ADP or oxygen, may not apply to

388   physiological intracellular conditions, relevant information is obtained in studies of kinetic

389   responses to conditions intermediate between the LEAK state at zero [ADP] and the OXPHOS

390   state at saturating [ADP], or of respiratory capacities in the range between kinetically saturating

391     $[O_2]$ and anoxia (Gnaiger 2001). We define respiratory capacities, comparable to channel

392   capacity in information theory, as the upper bound of the rate of respiration measured in defined

393   coupling and pathway control states of mitochondrial preparations (**Box 3**).

394
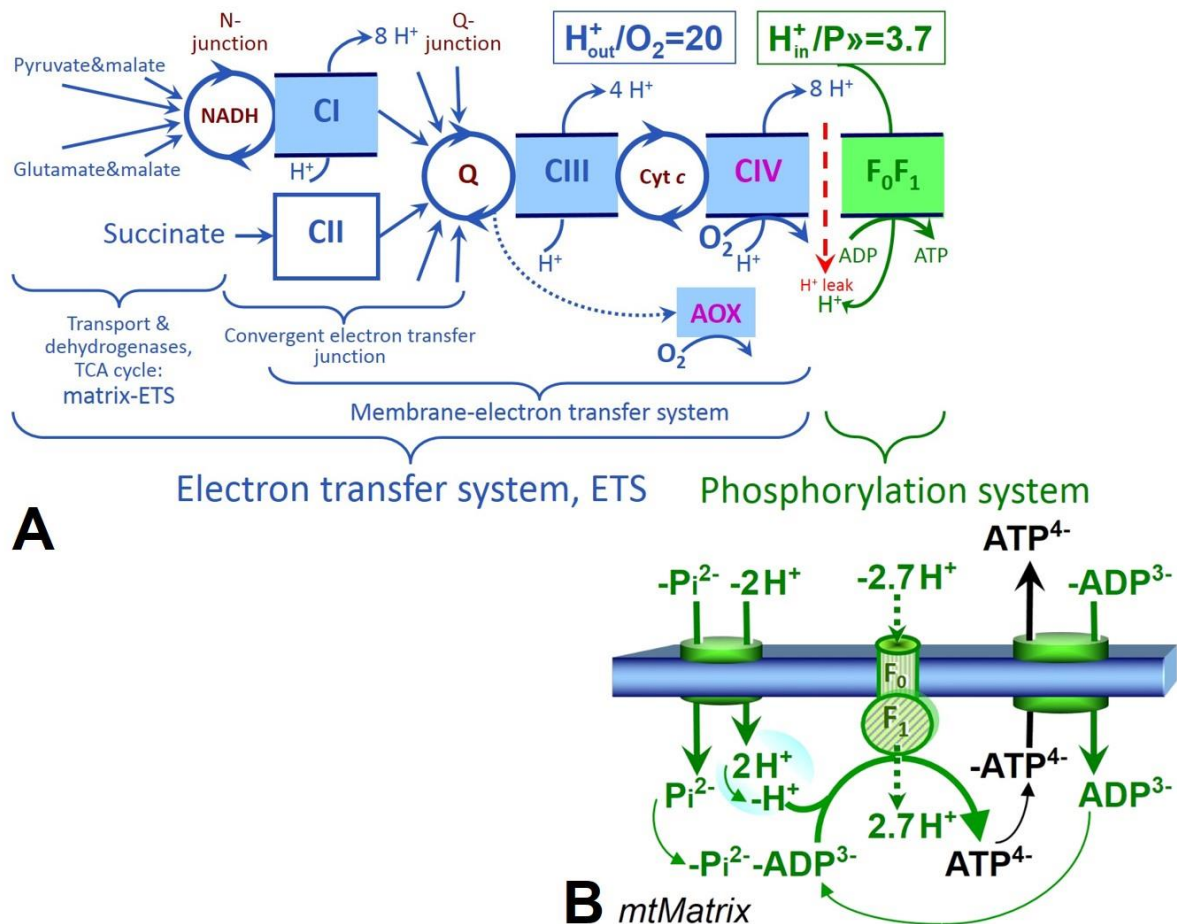
Fig. 1. The mitochondrial respiratory system and oxidative phosphorylation. (A) The electron transfer system, ETS, and coupling to the phosphorylation system. Multiple convergent electron transfer pathways are shown from NADH and succinate; additional arrows indicate electron entry through electron transferring flavoprotein, glycerophosphate dehydrogenase, dihydro-orotate dehydrogenase, choline dehydrogenase, and sulfide-ubiquinone oxidoreductase. The branched pathway of oxygen consumption by alternative quinol oxidase (AOX) is indicated by the dotted arrow. H^+_{out}/O_2 is the ratio of outward proton flux from the matrix space to catabolic O_2 flux in the NADH-linked pathway. $H^+_{in}/P»$ is the ratio of inward proton flux from the inter-membrane space to the flux of phosphorylation of ADP to ATP. Due to proton leak and slip these are not fixed stoichiometries. **(B)** Phosphorylation system consisting of the F_1F_0 ATP synthase, adenine nucleotide translocase, and the inorganic phosphate transporter. The $H^+_{in}/P»$ stoichiometry is the sum of the coupling stoichiometry in the ATP synthase reaction (-2.7 H^+ from the intermembrane space, 2.7 H^+ to the matrix) and the proton balance in the translocation of ADP^{2-}, ATP^{3-} and P_i^{2-}. See Eqs. 3 and 4 for further explanation. Modified from (A) Lemieux *et al.* (2017) and (B) Gnaiger (2014).
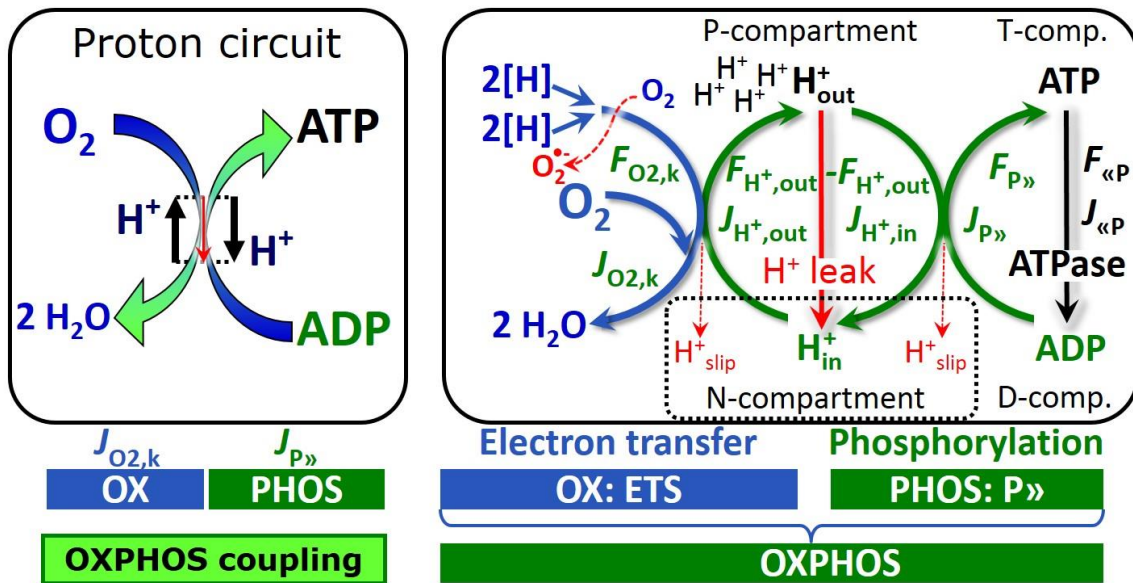
Fig. 2. The proton circuit and coupling in oxidative phosphorylation (OXPHOS). Oxygen flux, $J_{O2,k}$, in a catabolic reaction k is coupled to the phosphorylation of ADP to ATP, $J_{P»}$, by the proton pumps of the electron transfer system, ETS, pushing the outward proton flux, $J_{H+,out}$, and generating the output protonmotive force, $F_{H+,out}$. ATP synthase is coupled to inward proton flux, $J_{H+,in}$, to phosphorylate ADP with inorganic phosphate to ATP, driven by the input protonmotive force, $F_{H+,in}=-F_{H+,out}$. 2[H] indicates the reduced hydrogen equivalents of fuel substrates that provide the chemical input force, $F_{O2,k}$ [kJ/mol O_2], of the catabolic reaction k with oxygen (Gibbs energy of reaction per mole O_2 consumed in reaction k), typically in the range of -460 to -480 kJ/mol. The output force is given by the phosphorylation potential difference (ADP phosphorylated to ATP), $F_{P»}$, which varies *in vivo* ranging from about 48 to 62 kJ/mol under physiological conditions. Fluxes, J_B, and forces, F_B, are expressed in either chemical units, [mol·s^{-1}·m^{-3}] and [J·mol^{-1}] respectively, or electrical units, [C·s^{-1}·m^{-3}] and [J·C^{-1}] respectively, per volume, V [m^3], of the system. The system defined by the boundaries shown as a full black line is not a black box, but is analysed as a compartmental system. The negative compartment (N-compartment, enclosed by the dotted line) is the matrix space, separated from the positive compartment (P-compartment) by the inner mitochondrial membrane. ADP+P_i and ATP are the substrate- and product-compartments (scalar D- and T-comp.), respectively. Chemical potentials of all substrates and products involved in the scalar reactions are measured in the P-compartment for calculation of the scalar forces $F_{O2,k}$ and $F_{P»}=-F_{«P}$. Modified from Gnaiger (2014).

431   **Phosphorylation, P»:** *Phosphorylation* in the context of OXPHOS is defined as

432   phosphorylation of ADP to ATP. On the other hand, the term phosphorylation is used generally

433   in many different contexts, *e.g.* protein phosphorylation. This justifies consideration of a

434   symbol more discriminating and specific than P as used in the P/O ratio (phosphate to atomic

435   oxygen ratio), where P indicates phosphorylation of ADP to ATP or GDP to GTP. We propose

436   the symbol P» for the endergonic direction of phosphorylation ADP→ATP, and likewise the

437   symbol «P for the corresponding exergonic hydrolysis ATP→ADP (**Fig. 2**). ATP synthase is

438   the proton pump of the phosphorylation system (**Fig. 1B**). P» may also involve substrate-level

439   phosphorylation as part of the tricarboxylic acid cycle (succinyl-CoA ligase) and

440   phosphorylation of ADP catalyzed by phosphoenolpyruvate carboxykinase, adenylate kinase,

441   creatine kinase, hexokinase and nucleoside diphosphate kinase (NDPK). Kinase cycles are

442   involved in intracellular energy transfer and signal transduction for regulation of energy flux.

443   In isolated mammalian mitochondria ATP production catalyzed by adenylate kinase, 2ADP ↔

444   ATP + AMP, proceeds without fuel substrates in the presence of ADP (Komlódi and Tretter

445   2017). $J_{P»}/J_{O2,k}$ (P»/O_2) is two times the 'P/O' ratio of classical bioenergetics. The effective

446   P»/O_2 ratio is diminished by: (*1*) the proton leak across the inner mitochondrial membrane from

447   low pH in the P-phase to high pH in the N-phase (P, positive; N, negative); (*2*) cycling of other

448   cations; (*3*) proton slip in the proton pumps when a proton effectively is not pumped; and (*4*)

449   electron leak in the univalent reduction of oxygen (O_2; dioxygen) to superoxide anion radical

450   ($O_2^{•-}$).

451

452   **Box 3: Coupling, power and efficiency, at constant temperature and pressure**

453   Energetic coupling means that two processes of energy transformation are linked such that the

454   input power, P_{in}, is the driving element of the output power, P_{out}, and the out/input power ratio

455   is the efficiency. In general, power is work per unit time [J.s^{-1}=W]. When describing a system

456   with volume V without information on the internal structure, the output is defined as the *external*

457 work (exergy) performed by the *total* system on its environment. Such as system may be open

458 for any type of exchange, or closed and thus allowing only heat and work to be exchanged

459 across the system boundaries. This is the classical black box approach of thermodynamics. In

460 contrast, in a colourful compartmental analysis of *internal* energy transformations (**Fig. 2**), the

461 system is structured and described by definition of internal compartments (with information on

462 the heterogeneity of the system; **Box 2**) and analysis of separate parts, *i.e.* a sequence of *partial*

463 energy transformations, tr. In general, power per unit volume, P_{tr}/V [W.L^{-1}], is the product of a

464 volume-specific flux, J_{tr}, and its conjugated force, F_{tr}, and is closely linked to the dissipation

465 function using the terminology of irreversible thermodynamics (Prigogine 1967; Gnaiger

466 1993a,b). Output power of proton translocation and catabolic input power are (**Fig. 2**),

467 Output: $$P_{H+,out}/V = J_{H+,out} \cdot F_{H+,out}$$

468 Input: $$P_k/V = J_{O2,k} \cdot F_{O2,k}$$

469 $F_{O2,k}$ is the exergonic input force with a negative sign, and, $F_{H+,out}$, is the endergonic output

470 force with a positive sign (**Box 4**). Ergodynamic efficiency is the ratio of output/input power,

471 or the flux ratio times force ratio (Gnaiger 1993a,b),

472 $$\varepsilon = \frac{P_{H+,out}}{-P_k} = \frac{J_{H+,out}}{J_{O2,k}} \cdot \frac{F_{H+,out}}{-F_{O2,k}}$$

473 The concept of incomplete coupling relates exclusively to the first term, *i.e.* the flux ratio, or

474 H^+_{out}/O_2 ratio (**Fig. 1**). Likewise, respirometric definitions of the P»/O_2 ratio and biochemical

475 coupling efficiency (Section 3.2) consider flux ratios. In a completely coupled process, the

476 power efficiency, ε, depends entirely on the force ratio, ranging from zero efficiency at an

477 output force of zero, to the limiting output force and maximum efficiency of 1.0, when the total

478 power of the coupled process, $P_t=P_k+P_{H+,out}$, equals zero, and any net flows are zero at

479 ergodynamic equilibrium of a coupled process. Thermodynamic equilibrium is defined as the

480 state when all potentials (all forces) are dissipated and equilibrate towards their minima of zero.

481 In a fully or completely coupled process, output and input fluxes are directly proportional in a

482 fixed ratio technically defined as a stoichiometric relationship (a gear ratio in a mechanical

483 system). Such maximal stoichiometric output/input flux ratios are considered in OXPHOS

484 analysis as the upper limits or mechanistic H^+_{out}/O_2 and $P»/O_2$ ratios (**Fig. 1**).

485

486   **The steady-state:** Mitochondria represent a thermodynamically open system functioning

487 as a biochemical transformation system in non-equilibrium states. State variables (protonmotive

488 force; redox states) and metabolic fluxes (*rates*) are measured in defined mitochondrial

489 respiratory *states*. Strictly, steady states can be obtained only in open systems, in which changes

490 due to *internal* transformations, *e.g.*, O_2 consumption, are instantaneously compensated for by

491 *external* fluxes *e.g.*, O_2 supply, such that oxygen concentration does not change in the system

492 (Gnaiger 1993b). Mitochondrial respiratory states monitored in closed systems satisfy the

493 criteria of pseudo-steady states for limited periods of time, when changes in the system

494 (concentrations of O_2, fuel substrates, ADP, P_i, H^+) do not exert significant effects on metabolic

495 fluxes (respiration, phosphorylation). Such pseudo-steady states require respiratory media with

496 sufficient buffering capacity and kinetically saturating concentrations of substrates to be

497 maintained, and thus depend on the kinetics of the processes under investigation. Proton

498 turnover, $J_{\infty H+}$, and ATP turnover, $J_{\infty P}$, proceed in the steady-state at constant $F_{H+,out}$, when $J_{\infty H+}$

499 $= J_{H+,out} = J_{H+,in}$, and at constant $F_{P»}$, when $J_{\infty P} = J_{P»} = J_{«P}$ (**Fig. 2**).

500

501

502

503

504

505

506

507 **Table 1. Coupling states and residual oxygen consumption in mitochondrial**

508 **preparations in relation to respiration and phosphorylation rate, $J_{O2,k}$ and $J_{P»}$,**

509 **and protonmotive force, $F_{H+,out}$.** Coupling states are established at kinetically

510 saturating concentrations of fuel substrates and O_2.

State	$J_{O2,k}$	$J_{P»}$	$F_{H+,out}$	Inducing factors	Limiting factors
LEAK	L; low proton leak-dependent respiration;	0	max.	Proton leak, slip, and cation cycling	$J_{P»}=0$: (*1*) without ADP, L_N; (*2*) max. ATP/ADP ratio, L_T; or (*3*) inhibition of the ADP phosphorylation system, L_{Omy}
OXPHOS	P; high ADP-stimulated respiration	max.	high	Kinetically saturating [ADP] and [P_i]	$J_{P»}$ by phosphorylation system; or $J_{O2,k}$ by electron transfer system
ETS	E; max. noncoupled respiration	0	low	Optimal external uncoupler concentration for max. oxygen flux	$J_{O2,k}$ by electron transfer system
ROX	Rox; min. residual O_2 consumption	0	0	$J_{O2,Rox}$ in non-ETS oxidation reactions	Full inhibition of ETS or absence of fuel substrates

511
512
513 **LEAK state** (**Fig. 3**):

514 LEAK state is defined as a state

515 of mitochondrial respiration

516 when O_2 flux mainly

517 compensates for the proton leak

518 in the absence of ATP synthesis,

519 at kinetically saturating

520 concentrations of O_2 and

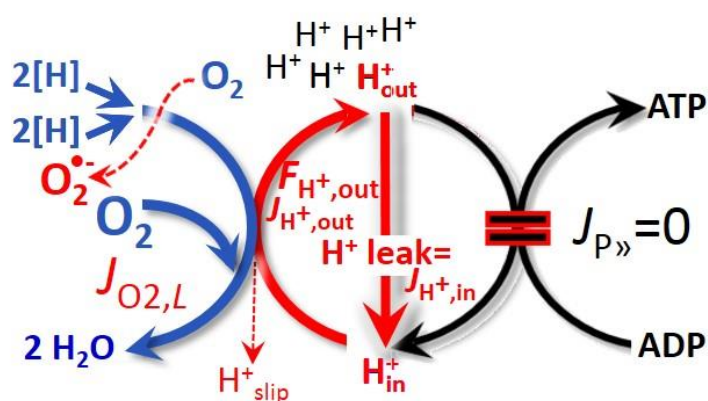521 respiratory substrates. LEAK

522 respiration is measured to obtain

Fig. 3. LEAK state: Phosphorylation is arrested, $J_{P»}=0$, and oxygen flux, $J_{O2,L}$, is controlled mainly by the proton leak, which equals $J_{H+,in}$, at maximum protonmotive force, $F_{H+,out}$ (See also Fig. 2).

523 an indirect estimate of *intrinsic uncoupling* without addition of any experimental uncoupler: (*1*)

524   in the absence of adenylates; (*2*) after depletion of ADP at maximum ATP/ADP ratio; or (*3*)

525   after inhibition of the phosphorylation system by inhibitors of ATP synthase, such as

526   oligomycin, or adenine nucleotide translocase, such as carboxyatractyloside.

527   **Proton leak:** Proton leak is the *uncoupled* process in which protons are translocated

528   across the inner mitochondrial membrane in the dissipative direction of the downhill

529   protonmotive force without coupling to phosphorylation (**Fig. 3**). The proton leak flux depends

530   on the protonmotive force, is a property of the inner mitochondrial membrane, may be enhanced

531   due to possible contaminations by free fatty acids, and is physiologically controlled. In

532   particular, uncoupling mediated by uncoupling protein 1 (UCP1) is physiologically controlled,

533   *e.g.*, in brown adipose tissue. UCP1 is a proton channel of the inner mitochondrial membrane

534   facilitating the conductance of protons across the inner mitochondrial membrane. As

535   consequence of this effective short-circuit, the protonmotive force diminishes, resulting in

536   stimulation of electron transfer to oxygen and heat dissipation without phosphorylation of ADP.

537   Mitochondrial injuries may lead to *dyscoupling* as a pathological or toxicological cause of

538   *uncoupled* respiration, *e.g.*, as a consequence of opening the permeability transition pore.

539   Dyscoupled respiration is distinguished from the experimentally induced *noncoupled*

540   respiration in the ETS state. Under physiological conditions, the proton leak is the dominant

541   contributor to the overall leak current.

542   **Proton slip:** Proton slip is the *decoupled* process in which protons are only partially

543   translocated by a proton pump of the ETS and slip back to the original compartment (Dufour *et*

544   *al.* 1996). Proton slip can also happen in association with the ATP-synthase, in which case the

545   proton slips downhill across the membrane to the matrix without contributing to ATP synthesis.

546   In each case, proton slip is a property of the proton pump and increases with the turnover rate

547   of the pump.

548   **Cation cycling:** Proton leak is a leak current of protons. There can be other cation

549   contributors to leak current including calcium and probably magnesium. Calcium current is

550   balanced by mitochondrial Na/Ca exchange, which is balanced by Na/H exchange or K/H

551   exchange. This is another effective uncoupling mechanism different from proton leak and slip.

552   Small differences of terms, *e.g.*, uncoupled, noncoupled, are easily overlooked and may

553   be erroneously perceived as identical. Even with an attempt at rigorous definition, the common

554   use of such terms may remain vague (**Table 2**).

555   **OXPHOS state** (**Fig. 4**):

556   OXPHOS state is defined as the

557   respiratory state with kinetically

558   saturating concentrations of O_2,

559   respiratory and phosphorylation

560   substrates, and absence of

561   exogenous uncoupler, which

562   provides an estimate of the

563   maximal capacity of OXPHOS in

564   any given pathway control state.
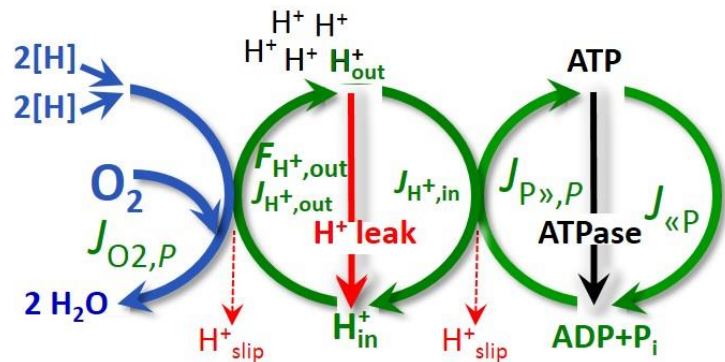
Fig. 4. OXPHOS state: Phosphorylation, $J_{P»}$, is stimulated by kinetically saturating [ADP] and inorganic phosphate, [P_i], and is supported by a high protonmotive force, $F_{H+,out}$. O_2 flux, $J_{O2,P}$, is highly coupled at a maximum P»/O_2 ratio, $J_{P»,P}/J_{O2,P}$ (See also Fig. 2).

565   Respiratory capacities at kinetically saturating substrate concentrations provide reference

566   values or upper limits of performance, aiming at the generation of data sets for comparative

567   purposes. Any effects of substrate kinetics are thus separated from reporting actual

568   mitochondrial capacity for oxidation during coupled respiration, against which physiological

569   activities can be evaluated.

570   As discussed previously, 0.2 mM ADP does not fully saturate flux in isolated

571   mitochondria (Gnaiger 2001; Puchowicz *et al.* 2004); greater ADP concentration is required,

572   particularly in permeabilized muscle fibres and cardiomyocytes, to overcome limitations by

573   intracellular diffusion and by the reduced conductance of the outer mitochondrial membrane

574   (Jepihhina *et al.* 2011, Illaste *et al.* 2012, Simson *et al.* 2016) either through interaction with

575   tubulin (Rostovtseva *et al.* 2008) or other intracellular structures (Birkedal *et al.* 2014). In

576   permeabilized muscle fibre bundles of high respiratory capacity, the apparent K_m for ADP

577   increases up to 0.5 mM (Saks *et al.* 1998), indicating that >90% saturation is reached only at

578   >5 mM ADP. Similar ADP concentrations are also required for accurate determination of

579   OXPHOS capacity in human clinical cancer samples and permeabilized cells (ref).

580

581   **Table 2. Distinction of terms related to coupling.**

Term	Respiration	P»/O₂	Note
Fully coupled	$P - L$	Max.	OXPHOS capacity corrected for LEAK respiration (**Fig. 6**)
Coupled	P	High	Phosphorylating respiration with a variable component of intrinsic LEAK respiration (**Fig. 4**)
Uncoupled, Decoupled	L	0	Non-phosphorylating respiration without added protonophore (**Fig. 3**)
Noncoupled	E	0	Non-phosphorylating respiration stimulated to maximum flux at optimum uncoupler concentration (**Fig. 5**)
Dyscoupled	P	Low	Pathologically increased uncoupling, mitochondrial dysfunction

582

583   **ETS state** (**Fig. 5**): The

584   ETS state is defined as the

585   *noncoupled* state with kinetically

586   saturating concentrations of O_2,

587   respiratory substrate and

588   optimum *exogenous* uncoupler

589   concentration for maximum O_2

590   flux, as an estimate of oxidative

591   ETS capacity. Inhibition of

Fig. 5. ETS state: Noncoupled respiration, $J_{O2,E}$, is maximum at optimum exogenous uncoupler concentration and phosphorylation is zero, $J_{P»}=0$ (See also Fig. 2).

592   respiration is observed at higher than optimum uncoupler concentrations. As a consequence of

593   the nearly collapsed protonmotive force, the driving force is insufficient for phosphorylation
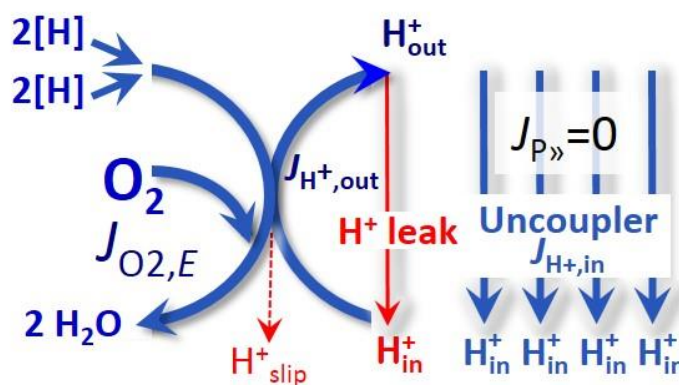
594   and $J_{P»}=0$.

595   Besides the three fundamental coupling states of mitochondrial preparations, the

596   following respiratory state also is relevant to assess respiratory function:

597   **ROX:** Residual oxygen consumption (ROX) is defined as O_2 consumption due to

598   oxidative side reactions remaining after inhibition of the ETS. ROX is not a coupling state but

599   represents a baseline that is used to correct mitochondrial respiration in defined coupling states.

600   ROX is not necessarily equivalent to non-mitochondrial respiration, considering oxygen-

601   consuming reactions in mitochondria not related to ETS, such as oxygen consumption in

602   reactions catalyzed by monoamine oxidases (type A and B), monooxygenases (cytochrome

603   P450 monooxygenases), dioxygenase (sulfur dioxygenase and trimethyllysine dioxygenase),

604   several hydoxylases, and more. Mitochondrial preparations, especially those obtained from

605   liver, are contaminated by peroxisomes. This fact makes the exact determination of

606   mitochondrial oxygen consumption and mitochondria-associated generation of reactive oxygen

607   species complicated (Schönfeld *et al.* 2009). The dependence of ROX-linked oxygen

608   consumption needs to be studied in detail with respect to non-ETS enzyme activities,

609   availability of specific substrates, oxygen concentration, and electron leakage leading to the

610   formation of reactive oxygen species.

611

612   *2.3. Coupling states and respiratory rates*

613   It is important to distinguish metabolic systems or modules from metabolic states and the

614   corresponding metabolic rates; for example: electron transfer system, ETS (**Fig. 6**), ETS state

615   (**Fig. 5**), and ETS capacity, *E*, respectively (**Table 1**). The protonmotive force is *high* in the

616   OXPHOS state when it drives phosphorylation, *maximum* in the LEAK state of coupled

617   mitochondria, driven by LEAK respiration at a minimum back flux of protons to the matrix

618   side, and *very low* in the ETS state when uncouplers short-circuit the proton cycle (**Table 1**).

Fig. 6. Four-compartment model of oxidative phosphorylation. Respiratory states (ETS, OXPHOS, LEAK) and corresponding rates (E, P, L) are connected by the protonmotive force, $F_{H+,out}$. Electron transfer system capacity, E, is partitioned into the dissipative LEAK respiration, L, partial conservation of the protonmotive exergy (**Box 4**) as the phosphorylation exergy in net OXPHOS capacity, P-L, and the excess capacity, E-P. Modified from Gnaiger (2014).
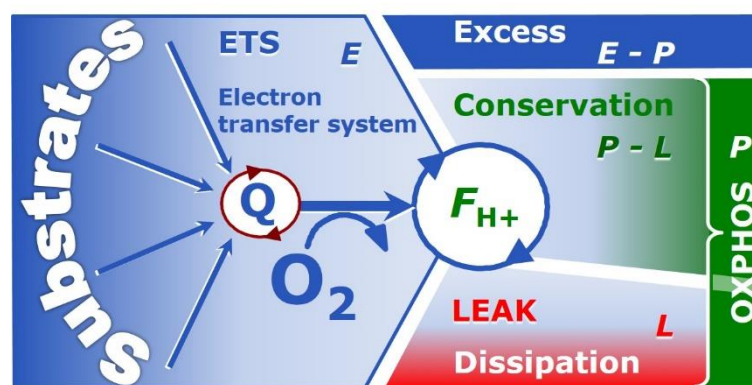
The three coupling states, ETS, LEAK and OXPHOS, are presented in a schematic context with the corresponding respiratory rates, abbreviated as E, L and P, respectively (**Fig. 6**). This clarifies that E may exceed or be equal to P, but E cannot theoretically be lower than P. $E<P$ must be discounted as an artefact, which may be caused experimentally by: (*1*) loss of oxidative capacity during the time course of the respirometric assay, since E is measured subsequently to P; (*2*) using too low uncoupler concentrations; (*3*) using high uncoupler concentrations which inhibit the ETS (Gnaiger 2008); (*4*) high oligomycin concentrations applied for measurement of L before titrations of uncoupler, when oligomycin exerts an inhibitory effect on E. On the other hand, the excess ETS capacity is overestimated if non-saturating [P_i] or [ADP] (State 3) are used.

$E>P$ is observed in many types of mitochondria, varying between species, tissues and cell types. It is the excess ETS capacity pushing the phosphorylation system (**Fig. 1B**) to the limit of its *capacity of utilizing* the protonmotive force. Within any type of mitochondria, the magnitude of $E>P$ depends on (*1*) the pathway control state with single or multiple electron input into the Q-junction and involvement of three or fewer coupling sites determining the H^+_{out}/O_2 *coupling stoichiometry* (**Fig. 1A**); and (*2*) the *biochemical coupling efficiency*

647   expressed as (*E-L)/E*, since an increase of *L* causes *P* to increase towards the limit of *E*. The

648   *excess E-P* capacity, *E-P*, therefore, provides a sensitive diagnostic indicator of specific injuries

649   of the phosphorylation system, under conditions when *E* remains constant but *P* declines

650   relative to controls (**Fig. 6**). Substrate cocktails supporting simultaneous convergent electron

651   transfer to the Q-junction for reconstitution of tricarboxylic acid cycle (TCA cycle) function

652   establish pathway control states with high ETS capacity, and consequently increase the

653   sensitivity of the *E-P* assay.

654   When subtracting *L* from *P*, the dissipative LEAK component in the OXPHOS state may

655   be overestimated. This can be avoided by measuring LEAK respiration in a state when the

656   protonmotive force is adjusted to its slightly lower value in the OXPHOS state, *e.g.*, by titration

657   of an ETS inhibitor. Any turnover-dependent components of proton leak and slip, however, are

658   underestimated under these conditions (Garlid *et al.* 1993). In general, it is inappropriate to use

659   the term *ATP production* for the difference of oxygen consumption measured in states *P* and *L*.

660   The difference *P-L* is the upper limit of the part of OXPHOS capacity that is freely available

661   for ATP production (corrected for LEAK respiration) and is fully coupled to phosphorylation

662   with a maximum mechanistic stoichiometry (**Fig. 6**).

663

664   *2.4. Classical terminology for isolated mitochondria*

665   *'When a code is familiar enough, it ceases appearing like a code; one forgets that*

666   *there is a decoding mechanism. The message is identical with its meaning'*

667   (Hofstadter 1979).

668   Chance and Williams (1955; 1956) introduced five classical states of mitochondrial respiration

669   and cytochrome redox states. **Table 3** shows a protocol with isolated mitochondria in a closed

670   respirometric chamber, defining a sequence of respiratory states.

671

672
673
674

Table 3. Metabolic states of mitochondria (Chance and Williams, 1956; Table V).

State	[O₂]	ADP level	Substrate level	Respiration rate	Rate-limiting substance
1	>0	low	low	Slow	ADP
2	>0	high	~0	Slow	Substrate
3	>0	high	high	Fast	respiratory chain
4	>0	low	high	Slow	ADP
5	0	high	high	0	Oxygen

675

676   **State 1** is obtained after addition of isolated mitochondria to air-saturated

677   isoosmotic/isotonic respiration medium containing inorganic phosphate, but no fuel substrates

678   and no adenylates, *i.e.*, AMP, ADP, ATP.

679   **State 2** is induced by addition of a high concentration of ADP (typically 100 to 300 µM),

680   which stimulates respiration transiently on the basis of endogenous fuel substrates and

681   phosphorylates only a small portion of the added ADP. State 2 is then obtained at a low

682   respiratory activity limited by zero endogenous fuel substrate availability (**Table 3**). If addition

683   of specific inhibitors of respiratory complexes, such as rotenone, does not cause a further

684   decline of oxygen consumption, State 2 is equivalent to residual oxygen consumption (See

685   below). If inhibition is observed, undefined endogenous fuel substrates are a confounding factor

686   of pathway control by externally added substrates and inhibitors. In contrast to the original

687   definition, an alternative protocol is frequently applied, in which State 2 is induced by addition

688   of fuel substrate without ADP (LEAK state), followed by addition of ADP.

689   **State 3** is the state stimulated by addition of fuel substrates while the ADP concentration

690   is still high (**Table 3**) and supports coupled energy transformation through oxidative

691   phosphorylation. 'High ADP' is a concentration of ADP specifically selected to allow the

692   measurement of State 3 to State 4 transitions of isolated mitochondria in a closed respirometric

693   system. Repeated ADP titration re-establishes State 3 at 'high ADP'. Starting at oxygen

694   concentrations near air-saturation (ca. 200 µM O_2 at sea level and 37 °C), the total ADP

695   concentration added must be low enough (typically 100 to 300 µM) to allow phosphorylation

to ATP at a coupled oxygen consumption that does not lead to oxygen depletion during the transition to State 4. In contrast, kinetically saturating ADP concentrations usually are an order of magnitude higher than 'high ADP', *e.g.* 2.5 mM in isolated mitochondria. The abbreviation State 3u is frequently used in bioenergetics, to indicate the state of respiration after titration of an uncoupler, without sufficient emphasis on the fundamental difference between OXPHOS capacity (*well-coupled* with an *endogenous* uncoupled component) and ETS capacity (*noncoupled*).

State 4 is a LEAK state which is obtained only if the mitochondrial preparation is intact and well-coupled. Depletion of ADP by phosphorylation to ATP leads to a decline in oxygen consumption in the transition from State 3 to State 4. Under these conditions, a maximum protonmotive force and high ATP/ADP ratio are maintained, and the P»/O_2 ratio can be calculated. State 4 respiration, L_T (**Table 1**), reflects intrinsic proton leak and intrinsic ATP hydrolysis activity. Oxygen consumption in State 4 is an overestimation of LEAK respiration if the contaminating ATP hydrolysis activity recycles some ATP to ADP, $J_{«P}$, which stimulates respiration coupled to phosphorylation, $J_{P»}>0$. This can be tested by inhibition of the phosphorylation system using oligomycin, ensuring that $J_{P»}=0$ (State 4o). Alternatively, sequential ADP titrations re-establish State 3, followed by State 3 to State 4 transitions while sufficient oxygen is available. However, anoxia may be reached before exhaustion of ADP (State 5).

State 5 is the state after exhaustion of oxygen in a closed respirometric chamber. Diffusion of oxygen from the surroundings into the aqueous solution may be a confounding factor preventing complete anoxia (Gnaiger 2001).

In **Table 3**, only States 3 and 4 (and 'State 2' in the alternative protocol without ADP; not included in the table) are coupling control states, with the restriction that O_2 flux in State 3 may be limited kinetically by non-saturating ADP concentrations (**Table 1**).

722 **3. States and rates**

723 *3.1. The protonmotive force and proton flux*

724   The protonmotive force across the inner mitochondrial membrane (Mitchell and Moyle

725 1967) was introduced most beautifully in the *Grey Book 1966* (see Mitchell 2011),

726 $$\Delta p_{H+} = \Delta\Psi + \Delta\mu_{H+}/F \qquad \text{(Eq. 1)}$$

727 The protonmotive force consists of two partial forces: (*1*) The electrical part, $\Delta\Psi$, is the

728 difference of charge (electric potential difference) and is not specific for H^+. (*2*) The chemical

729 part, $\Delta\mu_{H+}$, is the chemical potential difference in H^+, is proportional to the pH difference, and

730 incorporates the Faraday constant (**Table 4**).

731

732 **Table 4. Protonmotive force and flux matrix.** Rows: Electrical and chemical

733 isomorphic format (*e* and *n*). The Faraday constant, *F*, converts protonmotive force

734 and flux from *isomorphic format e* to *n*. Columns: The protonmotive force is the sum of

735 *partial isomorphic forces F*$_{el}$ and *F*$_{H+,d}$. In contrast to force (state), the conjugated flux

736 (rate) cannot be partitioned.
737

State		**Force**		**electric**	**+**	**chem.**	**Unit**	**Notes**
	Protonmotive force, *e*	Δp_{H+}	=	$\Delta\Psi$	+	$\Delta\mu_{H+}/F$	$J\cdot C^{-1}$	1*e*
	Chemiosmotic potential, *n*	$\Delta\widetilde{\mu}_{H+}$	=	$\Delta\Psi\cdot F$	+	$\Delta\mu_{H+}$	$J\cdot mol^{-1}$	1*n*
State	**Isomorphic force**	$F_{H+,out/i}$	=	**el**$_{out}$	+	$H^+_{out,d}$		
	Electric charge, *e*	$F_{H+,out/e}$	=	$F_{el,out/e}$	+	$F_{H+,out,d/e}$	$J\cdot C^{-1}$	2*e*
	Amount of substance, *n*	$F_{H+,out/n}$	=	$F_{el,out/n}$	+	$F_{H+,out,d/n}$	$J\cdot mol^{-1}$	2*n*
Rate	**Isomorphic flux**	$J_{H+,out/i}$	=	*e*	**or**	*n*		
	Electric charge, *e*	$J_{H+,out/e}$		$J_{H+,out/e}$			$C\cdot s^{-1}\cdot m^{-3}$	3*e*
	Amount of substance, *n*	$J_{H+,out/n}$				$J_{H+,out/n}$	$mol\cdot s^{-1}\cdot m^{-3}$	3*n*

738

739 1: The Faraday constant, *F*, is the product of elementary charge ($e=1.602177\cdot10^{-19}\cdot C$) and the

740   Avogadro (Loschmidt) constant ($N_A=6.022136\cdot10^{23}\cdot mol^{-1}$), $F=eN_A=96,485.3$ C/mol. $\Delta\widetilde{\mu}_{H+}$ is the

741   chemiosmotic potential difference. 1*e* and 1*n* are the classical representations of 2*e* and 2*n*.

742   2: The protonmotive force is $F_{\text{H+,out}}$, expressed either in isomorphic format e or n. $F_{\text{el}/e}\equiv\Delta\Psi$ is the partial

743   protonmotive force (el) acting generally on charged motive molecules (*i.e.* ions that are displaceable

744   across the inner mitochondrial membrane). In contrast, $F_{\text{H+,d}/n}\equiv\Delta\mu_{\text{H+}}$ is the partial protonmotive force

745   specific for proton displacement (H^+_d). The sign of the force is negative for exergonic transformations

746   in which exergy is lost or dissipated, and positive for endergonic transformations which conserve

747   exergy from a coupled exergonic process (**Box 4**).

748   3: The sign of the flux depends on the definition of the compartmental direction of the translocation (**Fig.**

749   **2**). Flux x force = $J_{\text{H+,out}/e}\cdot F_{\text{H+,out}/e} = J_{\text{H+,out}/n}\cdot F_{\text{H+,out}/n}$ = Volume-specific power [$J\cdot s^{-1}\cdot m^{-3}=W\cdot m^{-3}$].

Faraday constant, $F=eN_A$ [C/mol] (**Table 4**), enables the conversion between protonmotive force, $F_{\text{H+,out}/e}\equiv\Delta p_{\text{H+}}$ [J/C], expressed per *motive charge*, e [C], and protonmotive force or electrochemical potential difference, $F_{\text{H+,out}/n}\equiv\Delta\widetilde{\mu}_{\text{H+}}=\Delta p_{\text{H+}}\cdot F$ [J/mol], expressed per *motive amount of protons*, n [mol]. Proton charge, e, and amount of substance, n, define the units for the isomorphic formats. Taken together, F converts protonmotive force and flux from isomorphic format e to n (Eq. 2; see also **Table 4**, Note 2),

$$F_{\text{H+,out}/n} = F_{\text{H+,out}/e} \cdot eN_A \tag{Eq. 2.1}$$

$$J_{\text{H+,out}/n} = J_{\text{H+,out}/e} / (eN_A) \tag{Eq. 2.2}$$

In each format, the protonmotive force is expressed as the sum of two partial forces. The concept expressed by the complex symbols in Eq. 1 can be explained and visualized more easily by *partial isomorphic forces* as the components of the protonmotive force:

Electrical part of the protonmotive force: (*1*) Isomorph e: $F_{\text{el}/e}\equiv\Delta\Psi$ is the electrical part of the protonmotive force expressed in units joule per coulomb, *i.e.* volt [V=J/C]. $F_{\text{el}/e}$ is defined as partial Gibbs energy change per *motive elementary charge*, e [C], not specific for proton charge (**Table 4**, Note 2e). (*2*) Isomorph n: $F_{\text{el}/n}\equiv\Delta\Psi\cdot F$ is the electric force expressed in units joule per mole [J/mol], defined as partial Gibbs energy change per *motive amount of charge*, n [mol], not specific for proton charge (**Table 4**, Note 2n).

768   **Chemical part of the protonmotive force:** (*1*) Isomorph *n*: $F_{d,H+/n} \equiv \Delta\mu_{H+}$ is the chemical

769   part (diffusion, displacement of H^+) of the protonmotive force expressed in units joule per mole

770   [J/mol]. $F_{d,H+/n}$ is defined as partial Gibbs energy change per *motive amount of protons, n* [mol]

771   (**Table 4**, Note 2*n*). (*2*) Isomorph *e*: $F_{d,H+/e} \equiv \Delta\mu_{H+}/F$ is the chemical force expressed in units

772   joule per coulomb [V], defined as partial Gibbs energy change per *motive amount of protons*

773   *expressed in units of electric charge, e* [C], but specific for proton charge (**Table 4**, Note 2*e*).

774   Protonmotive means that there is a potential for the movement of protons, and force is a

775   measure of the potential for motion. Motion is relative and not absolute (Principle of Galilean

776   Relativity); likewise there is no absolute potential, but (isomorphic) forces are potential

777   differences. An electric partial force expressed in the format of electric charge, $F_{el/e}$, of -0.2 V

778   (**Table 5**, Note 5*e*) is equivalent to force in the format of amount, $F_{el,H+/n}$, of 19 kJ·mol^{-1} H^+_{out}

779   (Note 5*n*). For a ΔpH of 1 unit, the chemical partial force in the format of amount, $F_{d,H+/n}$,

780   changes by 5.9 kJ·mol^{-1} (**Table 5**, Note 6*n*) and chemical force in the format of charge $F_{d,H+/e}$

781   changes by 0.06 V (Note 6*e*). Considering a driving force of -470 kJ·mol^{-1} O_2 for oxidation, the

782   thermodynamic limit of the H^+_{out}/O_2 ratio is reached at a value of 470/19=24, compared to a

783   mechanistic stoichiometry of 20 (**Fig. 1**).

784

785   **Box 4: Endergonic and exergonic transformations, exergy and dissipation**

786   A chemical reaction, or any transformation, is exergonic if the Gibbs energy change (exergy)

787   of the reaction is negative at constant temperature and pressure. The sum of Gibbs energy

788   changes of all internal transformations in a system can only be negative, i.e. exergy is

789   irreversibly dissipated. Endergonic reactions are characterized by positive Gibbs energies of

790   reaction and cannot proceed spontaneously in the forward direction as defined. For instance,

791   the endergonic reaction P» is coupled to exergonic catabolic reactions, such that the total Gibbs

792   energy change is negative, *i.e.* exergy must be dissipated for the reaction to proceed (**Fig. 2**).

793   In contrast, energy cannot be lost or produced in any internal process, which is the key

794   message of the first law of thermodynamics. Thus mitochondria are the sites of energy

795   transformation but not energy production. Open and closed systems can gain energy and exergy

796   only by external fluxes, *i.e.* uptake from the environment. Exergy is the potential to perform

797   work. In the framework of flux-force relationships (**Box 3**), the *partial* derivative of Gibbs

798   energy per advancement of a transformation is an isomorphic force, F_{tr} (**Table 5**, Note 2). In

799   other words, force is equal to exergy/motive unit (in integral form, this definition takes care of

800   non-isothermal processes). This formal generalization represents an appreciation of the

801   conceptual beauty of Peter Mitchell's innovation of the protonmotive force against the

802   background of the established paradigm of the electromotive force (emf) defined at the limit of

803   zero current (Cohen *et al.* 2008).

804

805   **Table 5. Power, exergy, force, flux, and advancement.**
806

Expression	Symbol	Definition	Unit	Notes
Power, volume-specific	$P_{V,tr}$	$P_{V,tr} = J_{tr} \cdot F_{tr} = \partial_{tr}G \cdot \partial t^{-1}$	$W = J \cdot s^{-1} \cdot m^{-3}$	1
Force, isomorphic	F_{tr}	$F_{tr} = \partial_{tr}G \cdot \partial_{tr}\xi^{-1}$	$J \cdot x^{-1}$	2
Flux, isomorphic	J_{tr}	$J_{tr} = d_{tr}\xi \cdot dt^{-1} \cdot V^{-1}$	$x \cdot s^{-1} \cdot m^{-3}$	3
Advancement, n	$d_{tr}\xi_{H+/n}$	$d_{tr}\xi_{H+/n} = d_{tr}n_{H+} \cdot \nu_{H+}^{-1}$	mol	$4n$
Advancement, e	$d_{tr}\xi_{H+/e}$	$d_{tr}\xi_{H+/e} = d_{tr}e_{H+} \cdot \nu_{H+}^{-1}$	C	$4e$
Electric partial force, e	$F_{el/e}$	$F_{el/e} \equiv \Delta\Psi$	V	$5e$
Electric partial force, n	$F_{el/n}$	$\Delta\Psi \cdot F = 96.5 \cdot \Delta\Psi$	$kJ \cdot mol^{-1}$	$5n$
Chemical partial force, e	$F_{d,H+/e}$	$\Delta\mu_{H+}/F = -\ln(10) \cdot RT/F \cdot \Delta pH$	V	$6e$
at 37 °C		$= -0.06 \cdot \Delta pH$	$J \cdot C^{-1}$	
Chemical partial force, n	$F_{d,H+/n}$	$\Delta\mu_{H+} = -\ln(10) \cdot RT \cdot \Delta pH$	$J \cdot mol^{-1}$	$6n$
at 37 °C		$= -5.9 \cdot \Delta pH$	$kJ \cdot mol^{-1}$	

807

808   1 to 4: An isomorphic motive entity or transformant, expressed in units x, is defined for any

809   transformation, tr. x=mol or C in proton translocation.

810 2: $\partial_{tr}G$ [J] is the partial Gibbs energy change in the advancement of transformation tr.

811 3: For x=C, flow is electric current, I_{el} [A = C·s^{-1}], vector flux is electric current density per area, $\mathbf{J}_{el}$,

812   and compartmental flux is electric current density per volume, I_{el} [A·m^{-3}].

813 4n: For a chemical reaction, the advancement of reaction r is $d_r\xi_B = d_r n_B \cdot v_B^{-1}$ [mol]. The stoichiometric

814   number is v_B=-1 or v_B=1, depending on B being a product or substrate, respectively, in reaction r

815   involving one mole of B. The conjugated *intensive* molar quantity, $F_{B,r} = \partial_r G / \partial_r \xi_B$ [J·mol^{-1}], is the

816   chemical force of reaction or *reaction-motive* force per stoichiometric amount of B. In reaction

817   kinetics, $d_r n_B$ is expressed as a volume-specific quantity, which is the partial contribution to the

818   total concentration change of B, $d_r c_B = d_r n_B / V$ and $d c_B = d n_B / V$, respectively. In open systems with

819   constant volume V, $d c_B = d_r c_B + d_e c_B$, where r indicates the *internal* reaction and e indicates the

820   *external* flux of B into the unit volume of the system. At steady state the concentration does not

821   change, $d c_B$=0, when $d_r c_B$ is compensated for by the external flux of B, $d_r c_B = -d_e c_B$ (Gnaiger

822   1993b). Alternatively, $d c_B$=0 when B is held constant by different coupled reactions in which B

823   acts as a substrate or a product.

824 4e: Scalar potential difference across the mitochondrial membrane. In a scalar electric transformation

825   (flux of charge, *i.e.* volume-specific current, from the matrix space to the intermembrane and

826   extramitochondrial space) the motive force is the difference of charge (**Box 2**). The endergonic

827   direction of translocation is defined in **Fig. 2** as H$^+_{in}$ → H$^+_{out}$.

828 5n: F=96.5 (kJ·mol^{-1})/V.

829 6: The electric partial force is independent of temperature (Note 5), but the chemical partial force

830   depends on absolute temperature, T [K].

831 6e: RT is the gas constant times absolute temperature. $\ln(10)\cdot RT/F$ = 59.16 and 61.54 mV at 298.15

832   and 310.15 K (25 and 37 °C), respectively.

833 6n: $\ln(10)\cdot RT$ = 5.708 and 5.938 kJ·mol^{-1} at 298.15 and 310.15 K (25 and 37 °C), respectively.

834

835 *3.2. Forces and fluxes in physics and irreversible thermodynamics*

836   According to its definition in physics, a potential difference and as such the

837 *protonmotive force*, Δp_{H+}, is not a force *per se* (Cohen *et al.* 2008). The fundamental forces of

838 physics are distinguished from *motive forces* of statistical and irreversible thermodynamics.

839 Complementary to the attempt towards unification of fundamental forces defined in physics,

840 the concepts of Nobel laureates Lars Onsager, Erwin Schrödinger, Ilya Prigogine and Peter

841 Mitchell (even if expressed in apparently unrelated terms) unite the diversity of *generalized* or

842 'isomorphic' *flux-force* relationships, the product of which links to the dissipation function and

843 Second Law of thermodynamics (Schrödinger 1944; Prigogine 1967). A *motive force* is the

844 derivative of potentially available or 'free' energy (exergy) per isomorphic *motive* unit (**Box 4**).

845 Perhaps the first account of a *motive force* in energy transformation can be traced back to the

846 Peripatetic school around 300 BC in the context of moving a lever, up to Newton's motive force

847 proportional to the alteration of motion (Coopersmith 2010).

848   **Vectorial and scalar forces, and fluxes:** In chemical reactions and osmotic or diffusion

849 processes occurring in a closed heterogeneous system, such as a chamber containing isolated

850 mitochondria, scalar transformations occur without measured spatial direction but between

851 separate compartments (translocation between the matrix and intermembrane space) or between

852 energetically-separated chemical substances (reactions from substrates to products). Hence, the

853 corresponding fluxes are not vectorial but scalar, and are expressed per volume and not per

854 membrane area (**Box 2**). The corresponding motive forces are also scalar potential *differences*

855 across the membrane (**Table 5**), without taking into account the *gradients* across the 6 nm thick

856 inner mitochondrial membrane (Rich 2003).

857   **Coupling:** In energetics (ergodynamics), coupling is defined as an exergy transformation

858 fuelled by an exergonic (downhill) input process driving the advancement of an endergonic

859 (uphill) output process. The (negative) output/input power ratio is the efficiency of a coupled

860 energy transformation (**Box 3**). At the limit of maximum efficiency of a completely coupled

861 system, the (negative) input power equals the (positive) output power, such that the total power

862 approaches zero at the maximum efficiency of 1, and the process becomes fully reversible

863 without any dissipation of exergy, i.e. without entropy production.

864   **Coupled versus bound processes:** Since the chemiosmotic theory describes the

865 mechanisms of coupling in OXPHOS, it may be interesting to ask if the electrical and chemical

866   parts of proton translocation are coupled processes. This is not the case according to the

867   definition of coupling. If the coupling mechanism is disengaged, the output process becomes

868   independent of the input process, and both proceed in their downhill (exergonic) direction (**Fig.**

869   **2**). It is not possible to physically uncouple the electrical and chemical processes, which are

870   only *theoretically* partitioned as electrical and chemical components and can be measured

871   separately. If partial processes are non-separable, *i.e.*, cannot be uncoupled, then these are not

872   *coupled* but are defined as *bound* processes. The electrical and chemical parts are tightly bound

873   partial forces of the protonmotive force, since a flux cannot be partitioned but expressed only

874   in either an electrical or chemical isomorphic format (**Table 4**).

875

876   **4. Normalization: fluxes and flows**

877   *4.1. Flux per chamber volume*

878   The volume-specific *flux of a chemical reaction* r is the time derivative of the

879   advancement of the reaction per unit volume, $J_{V,B} = d_r\xi_B/dt \cdot V^{-1}$ [$(mol \cdot s^{-1}) \cdot L^{-1}$]. The *rate of*

880   *concentration change* is dc_B/dt [$(mol \cdot L^{-1}) \cdot s^{-1}$], where concentration is $c_B = n_B/V$. It is helpful to

881   make the subtle distinction between [$mol \cdot s^{-1} \cdot L^{-1}$] and [$mol \cdot L^{-1} \cdot s^{-1}$] for the fundamentally

882   different quantities of volume-specific flux and rate of concentration change, which merge to a

883   single expression only in closed systems. In open systems, external fluxes (such as O_2 supply)

884   are distinguished from internal transformations (metabolic flux, O_2 consumption). In a closed

885   system, external flows of all substances are zero and O_2 consumption (internal flow), I_{O2}

886   [$pmol \cdot s^{-1}$], causes a decline of the amount of O_2 in the system, n_{O2} [nmol]. Normalization of

887   these quantities for the volume of the system, V [$L = dm^3$], yields volume-specific O_2 flux,

888    $J_{V,O2} = I_{O2}/V$ [$nmol \cdot s^{-1} \cdot L^{-1}$], and O_2 concentration, [O_2] or $c_{O2} = n_{O2}/V$ [$nmol \cdot mL^{-1} = \mu mol \cdot L^{-1} = \mu M$].

889   Instrumental background O_2 flux is due to external flux into a non-ideal closed respirometer,

890   such that total volume-specific flux has to be corrected for instrumental background O_2 flux,

891   i.e. O_2 diffusion into or out of the instrumental chamber. $J_{V,O2}$ is relevant mainly for

892 methodological reasons and should be compared with the accuracy of instrumental resolution

893 of background-corrected flux, *e.g.* ±1 nmol·s^{-1}·L^{-1} (Gnaiger 2001). 'Metabolic' or catabolic

894 indicates O$_2$ flux, $J_{O2,k}$, corrected for instrumental background O$_2$ flux and chemical background

895 O$_2$ flux due to autoxidation of chemical components added to the incubation medium.
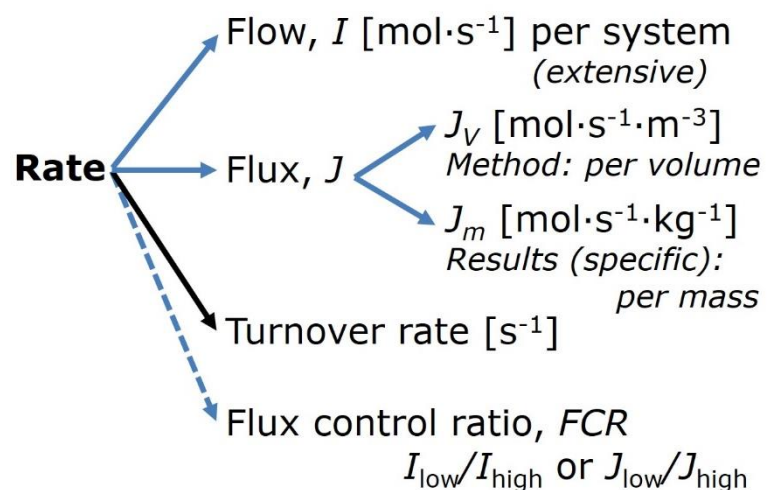
896

897 *4.2. Extensive quantities and size-specific normalization*

898 Application of common and generally defined units is required for direct transfer of

899 reported results into a database. The second [s] is the *SI* unit for the base quantity *time*. It is also

900 the standard time-unit used in solution chemical kinetics. **Table 6** lists some conversion factors

901 to obtain *SI* units. The term *rate* is not sufficiently defined to be useful for a database (**Fig. 7**).

902 The inconsistency of the meanings of rate becomes fully apparent when considering Galileo

903 Galilei's famous principle, that 'bodies of different weight all fall at the same rate (have a

904 constant acceleration)' (Coopersmith 2010).

905 **Extensive quantities:** An extensive quantity increases proportionally with system size.

906 The magnitude of an extensive quantity is completely additive for non-interacting subsystems,

907 such as mass or flow expressed per defined system. The magnitude of these quantities depends

908 on the extent or size of the system (Cohen *et al.* 2008).

909

910 **Fig. 7. Different meanings of *rate***

911 **may lead to confusion, if the**

912 **normalization is not sufficiently**

913 **specified.** Results are frequently

914 expressed as mass-specific *flux, J_m,*

915 per mg protein, dry or wet weight

916 (mass). Cell volume, V_{cell}, or

917 mitochondrial volume, V_{mt}, may be

918 used for normalization (volume-

Flow, I [mol·s^{-1}] per system
(extensive)

J_V [mol·s^{-1}·m^{-3}]
Method: per volume

Flux, J

J_m [mol·s^{-1}·kg^{-1}]
Results (specific):
per mass

Rate

Turnover rate [s^{-1}]

Flux control ratio, *FCR*
I_{low}/I_{high} or J_{low}/J_{high}

919 specific flux, $J_{V\text{cell}}$ or $J_{V\text{mt}}$), which then must be clearly distinguished from flux, J_V, expressed for

920 methodological reasons per volume of the measurement system, or flow per cell, I_X.

921

922   **Size-specific quantities:** 'The adjective *specific* before the name of an extensive quantity

923 is often used to mean *divided by mass*' (Cohen *et al.* 2008). Mass-specific flux is flow divided

924 by mass of the system. A mass-specific quantity is independent of the extent of non-interacting

925 homogenous subsystems. Tissue-specific quantities are of fundamental interest in comparative

926 mitochondrial physiology, where *specific* refers to the *type* rather than *mass* of the tissue. The

927 term *specific*, therefore, must be further clarified, such that tissue mass-specific, *e.g.*, muscle

928 mass-specific quantities are defined.

929   **Molar quantities:** 'The adjective *molar* before the name of an extensive quantity

930 generally means *divided by amount of substance*' (Cohen *et al.* 2008). The notion that all molar

931 quantities then become *intensive* causes ambiguity in the meaning of *molar Gibbs energy*. It is

932 important to emphasize the fundamental difference between normalization for amount of

933 substance *in a system* or for amount of motive substance *in a transformation*. When the Gibbs

934 energy of a system, G [J], is divided by the amount of substance B in the system, n_B [mol], a

935 *size-specific* molar quantity is obtained, $G_B = G/n_B$ [J·mol^{-1}], which is not any force at all. In

936 contrast, when the partial Gibbs energy change, $\partial_r G$ [J], is divided by the motive amount of

937 substance B in reaction r (advancement of reaction), $\partial_r \xi_B$ [mol], the resulting intensive molar

938 quantity, $F_{r,B} = \partial G/\partial_r \xi_B$ [J·mol^{-1}], is the chemical motive force of reaction r involving 1 mol B

939 (**Table 5**, Note 4).

940   **Flow per system, *I*:** In analogy to electrical terms, flow as an extensive quantity (*I*; per

941 system) is distinguished from flux as a size-specific quantity (*J*; per system size) (**Fig. 7**).

942 Electric current is flow, I_{el} [A=C·s^{-1}] per system (extensive quantity). When dividing this

943 extensive quantity by system size (membrane area), a size-specific quantity is obtained, which

944 is electric flux (electric current density), J_{el} [A·m^{-2} = C·s^{-1}·m^{-2}].

945   **Size-specific flux, *J***: Metabolic O_2 flow per tissue increases as tissue mass is increased.

946   Tissue mass-specific O_2 flux should be independent of the size of the tissue sample studied in

947   the instrument chamber, but volume-specific O_2 flux (per volume of the instrument chamber,

948   *V*) should increase in direct proportion to the amount of sample in the chamber. Accurate

949   definition of the experimental system is decisive: whether the experimental chamber is the

950   closed, open, isothermal or non-isothermal *system* with defined volume as part of the

951   measurement apparatus, in contrast to the experimental *sample* in the chamber (**Table 6**).

952   Volume-specific O_2 flux depends on mass-concentration of the sample in the chamber, but

953   should be independent of the chamber volume. There are practical limitations to increasing the

954   mass-concentration of the sample in the chamber, when one is concerned about crowding

955   effects and instrumental time resolution.

956   **Sample concentration C_{mX}:** Normalization for sample concentration is required for

957   reporting respiratory data. Consider a tissue or cells as the sample, *X*, and the sample mass, m_X

958   [mg] from which a mitochondrial preparation is obtained. The sample mass is frequently

959   measured as wet or dry weight ($m_X \equiv W_w$ or W_d [mg]), or as amount of tissue or cell protein

960   ($m_X \equiv m_{Protein}$). In the case of permeabilized tissues, cells, and homogenates, the sample

961   concentration, $C_{mX} = m_X/V$ [mg·mL^{-1}=g·L^{-1}], is simply the mass of the subsample of tissue that is

962   transferred into the instrument chamber. Part of the mitochondria from the tissue is lost during

963   preparation of isolated mitochondria, and only a fraction of mitochondria is obtained, expressed

964   as the mitochondrial yield (**Fig. 8**). At a high mitochondrial yield the sample of isolated

965   mitochondria is more representative of the total mitochondrial population than in preparations

966   characterized by low mitochondrial yield. Determination of the mitochondrial yield is based on

967   measurement of the concentration of a mitochondrial marker in the tissue homogenate, $C_{mte,thom}$,

968   which simultaneously provides information on the specific mitochondrial density in the sample

969   (**Fig. 8**).

970   Tissues can contain multiple cell populations which may have distinct mitochondrial

971   subtypes. Mitochondria are also in a constant state of flux due to highly dynamic fission and

972   fusion cycles, and can exist in multiple stages and sizes which may be altered by a range of

973   factors. The isolation of mitochondria (often achieved through differential centrifugation) can

974   therefore yield a subsample of the mitochondrial types present in a tissue, dependent on

975   isolation protocols utilized (e.g. centrifugation speed). This possible artefact should be taken

976   into account when planning experiments using isolated mitochondria. The tendency for

977   mitochondria of specific sizes to be enriched at different centrifugation speeds also has the

978   potential to allow the isolation of specific mitochondrial subpopulations and therefore the

979   analysis of mitochondria from multiple cell lineages within a single tissue.
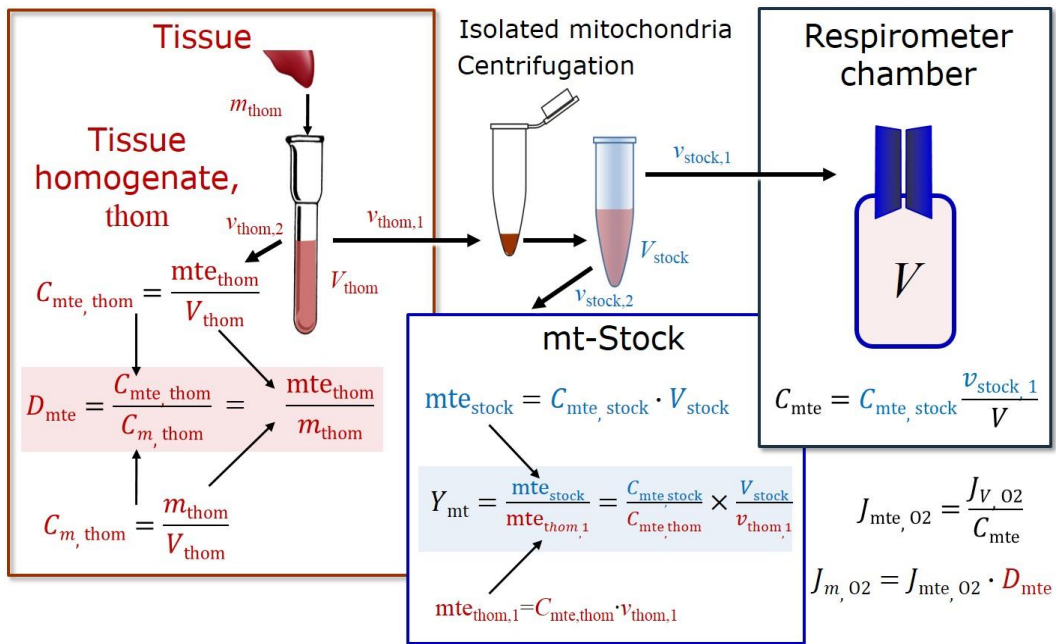
980

981
982 **Table 6. Sample concentrations and normalization of flux with *SI* base units.**

Expression	Symbol	Definition	*SI* Unit	Notes
Sample				
Identity of sample	X	Cells, animals, patients		
Number of sample entities X	N_X	Number of cells, *etc.*	x	
Mass of sample X	m_X		kg	1
Mass of entity X	M_X	$M_X = m_X \cdot N_X^{-1}$	$kg \cdot x^{-1}$	1
Mitochondria				
Mitochondria	mt	$X = mt$		
Amount of mt-elements	mte	Quantity of mt-marker	x_{mte}	
Concentrations				
Sample number concentration	C_{NX}	$C_{NX} = N_X \cdot V^{-1}$	$x \cdot m^{-3}$	2
Sample mass concentration	C_{mX}	$C_{mX} = m_X \cdot V^{-1}$	$kg \cdot m^{-3}$	
Mitochondrial concentration	C_{mte}	$C_{mte} = mte \cdot V^{-1}$	$x_{mte} \cdot m^{-3}$	3
Specific mitochondrial density	D_{mte}	$D_{mte} = mte \cdot m_X^{-1}$	$x_{mte} \cdot kg^{-1}$	4
Mitochondrial content, mte per entity X	mte_X	$mte_X = mte \cdot N_X^{-1}$	$x_{mte} \cdot x^{-1}$	5
O₂ flow and flux				6
Flow	I_{O2}	Internal flow	$mol \cdot s^{-1}$	7
Volume-specific flux	$J_{V,O2}$	$J_{V,O2} = I_{O2} \cdot V^{-1}$	$mol \cdot s^{-1} \cdot m^{-3}$	8
Flow per sample entity X	$I_{X,O2}$	$I_{X,O2} = J_{V,O2} \cdot C_{NX}^{-1}$	$mol \cdot s^{-1} \cdot x^{-1}$	9
Mass-specific flux	$J_{mX,O2}$	$J_{mX,O2} = J_{V,O2} \cdot C_{mX}^{-1}$	$mol \cdot s^{-1} \cdot kg^{-1}$	
Mitochondria-specific flux	$J_{mte,O2}$	$J_{mte,O2} = J_{V,O2} \cdot C_{mte}^{-1}$	$mol \cdot s^{-1} \cdot x_{mte}^{-1}$	10

983

984 1 The *SI* prefix k is used for the SI base unit of mass (kg=1,000 g). In praxis, various *SI* prefixes are

985   used for convenience, to make numbers easily readable, *e.g.* 1 mg tissue, cell or mitochondrial mass

986   instead of 0.000001 kg.

987 2 In case *X*=cells, the sample number concentration is $C_{Ncell}=N_{cell} \cdot V^{-1}$, and volume may be expressed

988   in [dm^3=L] or [cm^3=mL]. See Table 7 for different sample types.

989 3 mt-concentration is an experimental variable, dependent on sample concentration: (*1*) C_{mte}=mte$\cdot V^{-1}$;

990   (*2*) C_{mte}=mte$_X \cdot C_{NX}$; (*3*) $C_{mte}=C_{mX} \cdot D_{mte}$.

991 4 If the amount of mitochondria, mte, is expressed as mitochondrial mass, then D_{mte} is the mass

992   fraction of mitochondria in the sample. If mte is expressed as mitochondrial volume, V_{mt}, and the

993   mass of sample, m_X, is replaced by volume of sample, V_X, then D_{mte} is the volume fraction of

994   mitochondria in the sample.

995 5 mte$_X$=mte$\cdot N_X^{-1}=C_{mte} \cdot C_{NX}^{-1}$.

996 6 Entity O_2 can be replaced by other chemical entities B to study different reactions.

997 7 I_{O2} and *V* are defined per instrument chamber as a system of constant volume (and constant

998   temperature), which may be closed or open. I_{O2} is abbreviated for $I_{O2,r}$, *i.e.* the metabolic or internal

999   O_2 flow of the chemical reaction r in which O_2 is consumed, hence the negative stoichiometric

1000   number, v_{O2}=-1. $I_{O2,r}$=d$_r n_{O2}$/d$t \cdot v_{O2}^{-1}$. If r includes all chemical reactions in which O_2 participates, then

1001   d$_r n_{O2}$ = dn_{O2} – d$_e n_{O2}$, where dn_{O2} is the change in the amount of O_2 in the instrument chamber and

1002   d$_e n_{O2}$ is the amount of O_2 added externally to the system. At steady state, by definition dn_{O2}=0, hence

1003   d$_r n_{O2}$=–d$_e n_{O2}$.

1004 8 $J_{V,O2}$ is an experimental variable, expressed per volume of the instrument chamber.

1005 9 $I_{X,O2}$ is a physiological variable, depending on the size of entity *X*.

1006 10 There are many ways to normalize for a mitochondrial marker, that are used in different experimental

1007   approaches: (*1*) $J_{mte,O2} = J_{V,O2} \cdot C_{mte}^{-1}$; (*2*) $J_{mte,O2} = J_{V,O2} \cdot C_{mX}^{-1} \cdot D_{mte}^{-1} = J_{mX,O2} \cdot D_{mte}^{-1}$; (*3*) $J_{mte,O2} =$

1008 $J_{V,O2} \cdot C_{NX}^{-1} \cdot$ mte$_X^{-1} = I_{X,O2} \cdot$ mte$_X^{-1}$; (*4*) $J_{mte,O2} = I_{O2} \cdot$ mte^{-1}.

1009

1010

1011

1012

1013

Fig. 8. Normalization of volume-specific flux of isolated mitochondria and tissue homogenate. A: Mitochondrial yield, Y_{mt}, in preparation of isolated mitochondria. $v_{thom,1}$ and $v_{stock,1}$ are the volumes transferred from the total volume, V_{thom} and V_{stock}, respectively. $mte_{thom,1}$ is the amount of mitochondrial elements in volume $v_{thom,1}$ used for isolation. B: In respirometry with homogenate, $v_{thom,1}$ is transferred directly into the respirometer chamber. See Table 6 for further explanation of symbols.

Table 7. Some useful abbreviations

of various sample types, *X*.

_____

Identity of sample	*X*

_____

Mitochondrial preparations	mtprep
Isolated mitochondria	imt
Tissue homogenate	thom
Permeabilized tissue	pti
Permeabilized fibres	pfi
Permeabilized cells	pce
Cells	ce

_____

Mass-specific flux, $J_{mX,O2}$: Mass-specific flux is obtained by expressing respiration per mass of sample, m_X [mg]. *X* is the type of sample, *e.g.*, tissue homogenate, permeabilized fibres or cells. Volume-specific flux is divided by mass concentration of *X*, $J_{mX,O2} = J_{V,O2}/C_{mX}$; or flow per cell is divided by mass per cell, $J_{mcell,O2} = I_{cell,O2}/M_{cell}$. If mass-specific O_2 flux is constant and independent of sample size (expressed as mass), then there is no interaction between the subsystems. A 1.5 mg and a 3.0 mg muscle sample respires at identical mass-specific flux. Mass-specific O_2 flux, however, may change with the mass of a tissue sample, cells or isolated mitochondria in the measuring chamber, in which case the nature of the interaction becomes an issue. Optimization of cell density and arrangement is generally important and particularly in experiments carried out in wells, considering the confluency of the cell monolayer or clumps of cells (Salabei *et al.* 2014).

Number concentration, C_{NX}: The experimental *number concentration* of sample in the case of cells or animals, *e.g.*, nematodes is $C_{NX}=N_X/V$ [x·mL^{-1}], where N_X is the number of cells or organisms in the chamber (**Table 6**).

1053   **Flow per sample entity, $I_{X,O2}$:** A special case of normalization is encountered in

1054   respiratory studies with permeabilized (or intact) cells. If respiration is expressed per cell, the

1055 O_2 flow per measurement system is replaced by the O_2 flow per cell, $I_{cell,O2}$ (**Table 6**). O_2 flow

1056   can be calculated from volume-specific O_2 flux, $J_{V,O2}$ [nmol·s^{-1}·L^{-1}] (per V of the measurement

1057   chamber [L]), divided by the number concentration of cells, $C_{Nce}=N_{ce}/V$ [cell·L^{-1}], where N_{ce} is

1058   the number of cells in the chamber. Cellular O_2 flow can be compared between cells of identical

1059   size. To take into account changes and differences in cell size, further normalization is required

1060   to obtain cell size-specific or mitochondrial marker-specific O_2 flux (Renner *et al.* 2003).

1061   The complexity changes when the sample is a whole organism studied as an experimental

1062   model. The well-established scaling law in respiratory physiology reveals a strong interaction

1063   of O_2 consumption and individual body mass of an organism, since *basal* metabolic rate (flow)

1064   does not increase linearly with body mass, whereas *maximum* mass-specific O_2 flux, $\dot{V}_{O2max}$ or

1065 $\dot{V}_{O2peak}$, is approximately constant across a large range of individual body mass (Weibel and

1066   Hoppeler 2005), with individuals, breeds, and certain species deviating substantially from this

1067   general relationship. $\dot{V}_{O2peak}$ of human endurance athletes is 60 to 80 mL O_2·min^{-1}·kg^{-1} body

1068   mass, converted to $J_{m,O2peak}$ of 45 to 60 nmol·s^{-1}·g^{-1} (Gnaiger 2014; **Table 8**).

1069

1070   *4.2. Normalization for mitochondrial content*

1071   Normalization is a problematic subject and it is essential to consider the question of the

1072   study. If the study aims to compare tissue performance, such as the effects of a certain treatment

1073   on a specific tissue, then normalization can be successful, using tissue mass or protein content,

1074   for example. If the aim, however, is to find differences of mitochondrial function independent

1075   of mitochondrial density (**Table 6**), then normalization to a mitochondrial marker is imperative.

1076   However, one cannot assume that quantitative changes in various markers such as

1077   mitochondrial proteins necessarily occur in parallel with one another. It is important to first

1078   establish that the marker chosen is not selectively altered by the performed treatment. In

1079 conclusion, the normalization must reflect the question under investigation to reach a satisfying

1080 answer. On the other hand, the goal of comparing results across projects and institutions

1081 requires some standardization on normalization for entry into a databank.

1082 **Mitochondrial concentration, C_{mte}, and mitochondrial markers:** It is important that

1083 mitochondrial content in the tissue and the measurement chamber be quantified, as a

1084 physiological output and result of mitochondrial biogenesis and degradation, and as a quantity

1085 for normalization in functional analyses. Mitochondrial organelles comprise a cellular

1086 reticulum that is in a continual flux of fusion and fission. Hence the definition of an "amount"

1087 of mitochondria is often misconceived: mitochondria cannot be counted as a number of

1088 occurring elements. Therefore, quantification of the "amount" of mitochondria depends on

1089 measurement of chosen mitochondrial markers. 'Mitochondria are the structural and functional

1090 elemental units of cell respiration' (Gnaiger 2014). The quantity of a mitochondrial marker can

1091 be considered as the measurement of the amount of *elemental mitochondrial units* or

1092 *mitochondrial elements*, mte. However, since mitochondrial quality changes under certain

1093 stimuli, particularly in mitochondrial dysfunction, some markers can vary while other markers

1094 are unchanged. (*1*) Mitochondrial volume or membrane area are structural markers, whereas

1095 mitochondrial protein mass is frequently used as a marker for isolated   mitochondria.   (*2*)

1096 Mitochondrial marker enzymes (amounts or activities) and molecular markers can be selected

1097 as matrix markers, *e.g.*, citrate synthase activity, mtDNA; or inner mt-membrane markers, *e.g.*,

1098 cytochrome *c* oxidase activity, aa_3 content, cardiolipin, TOM20. (*3*) Extending the

1099 measurement of mitochondrial marker enzyme activity to mitochondrial pathway capacity,

1100 measured as ETS or OXPHOS capacity, can be considered as an integrative functional

1101 mitochondrial marker.

1102 Depending on the type of mitochondrial marker, the mitochondrial elements, mte, are

1103 expressed in marker-specific units. Although concentration and density are used synonymously

1104 in physical chemistry, it is recommended to distinguish *experimental mitochondrial*

1105   *concentration*, C_{mte}=mte/V and *physiological mitochondrial density*, D_{mte}= mte/m_X. Then

1106   mitochondrial density is the amount of mitochondrial elements per mass of tissue. The former

1107   is mitochondrial density multiplied by sample mass concentration, C_{mte}=D_{mte}·C_{mX}, or

1108   mitochondrial content multiplied by sample number concentration, C_{mte}=mte$_X$·C_{NX} (**Table 6**).

1109   **Mitochondria-specific flux, $J_{mte,O2}$**: Volume-specific metabolic O_2 flux depends on: (*1*)

1110   the sample concentration in the volume of the instrument chamber, C_{mX}, or C_{NX}; (*2*) the

1111   mitochondrial density in the sample, D_{mte}=mte/m_X or mte$_X$=mte/N_X; and (*3*) the specific

1112   mitochondrial activity or performance per elemental mitochondrial unit, $J_{mte,O2}$=$J_{V,O2}$/C_{mte}

1113   (**Table 6**). Obviously, the numerical results for $J_{mte,O2}$ vary according to the type of

1114   mitochondrial marker chosen for measurement of mte and C_{mte}=mte/V. Some problems are

1115   common for all mitochondrial markers: (*1*) Accuracy of measurement is crucial, since even a

1116   highly accurate and reproducible measurement of O_2 flux becomes inaccurate and noisy if

1117   normalized for a biased and noisy measurement of a mitochondrial marker. This problem is

1118   acute in mitochondrial respiration because the denominators used (the mitochondrial marker)

1119   are often very small moieties whose accurate and precise determination is difficult. This

1120   problem can be avoided when O_2 fluxes measured in substrate-uncoupler-inhibitor titration

1121   protocols are normalized for flux in a defined respiratory reference state, which is used as an

1122   *internal* marker and yields flux control ratios, *FCR*s (**Fig. 7**). *FCR*s are independent of any

1123   *externally* measured markers and, therefore, are statistically very robust. *FCR*s indicate

1124   qualitative changes of mitochondrial respiratory control, with highest quantitative resolution,

1125   separating the effect of mitochondrial density or concentration on $J_{mX,O2}$ or $I_{X,O2}$ from that of

1126   function per elemental mitochondrial marker, $J_{mte,O2}$ (Pesta *et al.* 2011; Gnaiger 2014). (*2*) If

1127   mitochondrial quality does not change and only the amount of mitochondria, defined by the

1128   chosen mitochondrial marker, varies as a determinant of mass-specific flux, then any marker is

1129   equally qualified and selection of the optimum marker depends only on the accuracy and

1130   precision of measurement of the mitochondrial marker. (*3*) If mitochondrial flux control ratios

1131   change, then there may not be any best mitochondrial marker. In general, measurement of

1132   multiple mitochondrial markers enables a comparison and evaluation of normalization for a

1133   variety of mitochondrial markers.

1134

1135   *4.3. Conversion: units and normalization*

1136   Many different units have been used to report the rate of oxygen consumption, OCR

1137   (**Table 8**). *SI* base units provide the common reference for introducing the theoretical principles

1138   (**Fig. 7**), and are used with appropriately chosen *SI* prefixes to express numerical data in the

1139   most practical format, with an effort towards unification within specific areas of application

1140   (**Table 9**). For studies of cells, we recommend that respiration be expressed, as far as possible,

1141   as (*1*) O_2 flux normalized for a mitochondrial marker, for separation of the effects of

1142   mitochondrial quality and content on cell respiration (this includes *FCR*s as a normalization for

1143   a functional mitochondrial marker); (*2*) O_2 flux in units of cell volume or mass, for comparison

1144   of respiration of cells with different cell size (Renner *et al.* 2003) and with studies on tissue

1145   preparations, and (*3*) O_2 flow in units of attomole (10^{-18} mol) of O_2 consumed by each cell in a

1146   second [$amol \cdot s^{-1} \cdot cell^{-1}$], numerically equivalent to [$pmol \cdot s^{-1} \cdot 10^{-6}$ cells]. This convention allows

1147   information to be easily used when designing experiments in which oxygen consumption must

1148   be considered. For example, to estimate the volume-specific O_2 flux in an instrument chamber

1149   that would be expected at a particular cell number concentration, one simply needs to multiply

1150   the flow per cell by the number of cells per volume of interest. This provides the amount of O_2

1151   [mol] consumed per time [s^{-1}] per unit volume [L^{-1}]. At an O_2 flow of 100 $amol \cdot s^{-1} \cdot cell^{-1}$ and a

1152   cell density of 10^9 $cells \cdot L^{-1}$ (10^6 $cells \cdot mL^{-1}$), the volume-specific O_2 flux is 100 $nmol \cdot s^{-1} \cdot L^{-1}$ (100

1153 $pmol \cdot s^{-1} \cdot mL^{-1}$). Although volume is expressed as m^3 using the *SI* base unit, the litre [dm^3] is the

1154   basic unit of volume for concentration and is used for most solution chemical kinetics. If one

1155   multiplies $I_{cell,O2}$ by C_{Ncell}, then the result will not only be the amount of O_2 [mol] consumed per

1156   time [s^{-1}] in one litre [L^{-1}], but also the change in the concentration of oxygen per second (for

1157 any volume of an ideally closed system). This is ideal for kinetic modeling as it blends with

1158 chemical rate equations where concentrations are typically expressed in $mol \cdot L^{-1}$ (Wagner *et al.*

1159 2011). In studies of multinuclear cells, such as differentiated skeletal muscle cells, it is easy to

1160 determine the number of nuclei but not the total number of cells. A generalized concept,

1161 therefore, is obtained by substituting cells by nuclei as the sample entity. This does not hold,

1162 however, for enucleated platelets.

1163

1164 **Table 8. Conversion of various units used in respirometry and**

1165 **ergometry.** e is the number of electrons or reducing equivalents. z_B is the

1166 charge number of entity B.

1167

1 Unit	x	Multiplication factor	*SI*-Unit	Note
ng.atom $O \cdot s^{-1}$	(2 e)	0.5	nmol $O_2 \cdot s^{-1}$	
ng.atom $O \cdot min^{-1}$	(2 e)	8.33	pmol $O_2 \cdot s^{-1}$	
natom $O \cdot min^{-1}$	(2 e)	8.33	pmol $O_2 \cdot s^{-1}$	
nmol $O_2 \cdot min^{-1}$	(4 e)	16.67	pmol $O_2 \cdot s^{-1}$	
nmol $O_2 \cdot h^{-1}$	(4 e)	0.2778	pmol $O_2 \cdot s^{-1}$	
mL $O_2 \cdot min^{-1}$ at STPD^a		0.744	µmol $O_2 \cdot s^{-1}$	1
W = J/s at -470 kJ/mol O_2		-2.128	µmol $O_2 \cdot s^{-1}$	
mA = mC$\cdot s^{-1}$	(z_{H+}=1)	10.36	nmol $H^+ \cdot s^{-1}$	2
mA = mC$\cdot s^{-1}$	(z_{O2}=4)	2.59	nmol $O_2 \cdot s^{-1}$	2
nmol $H^+ \cdot s^{-1}$	(z_{H+}=1)	0.09649	mA	3
nmol $O_2 \cdot s^{-1}$	(z_{O2}=4)	0.38594	mA	3

1168

1169 1 At standard temperature and pressure dry (STPD: 0 °C=273.15 K and 1

1170 atm=101.325 kPa=760 mmHg), the molar volume of an ideal gas, V_m, and $V_{m,O2}$

1171 is 22.414 and 22.392 $L.mol^{-1}$ respectively. Rounded to three decimal places, both

1172 values yield the conversion factor of 0.744. For comparison at NTPD (20 °C),

1173 $V_{m,O2}$ is 24.038 $L.mol^{-1}$. Note that the *SI* standard pressure is 100 kPa.

1174   2 The multiplication factor is $10^6/(z_B \cdot F)$.

1175   3 The multiplication factor is $z_B \cdot F/10^6$.

1176

1177 **Table 9. Conversion for units with preservation of numerical values.**

Name	Frequently used unit	Equivalent unit	Note
Volume-specific flux, $J_{V,O2}$	$pmol \cdot s^{-1} \cdot mL^{-1}$	$nmol \cdot s^{-1} \cdot L^{-1}$	1
	$mmol \cdot s^{-1} \cdot L^{-1}$	$mol \cdot s^{-1} \cdot m^{-3}$	
Cell-specific flow, I_{O2}	$pmol \cdot s^{-1} \cdot 10^{-6}$ cells	$amol \cdot s^{-1} \cdot cell^{-1}$	2
	$pmol \cdot s^{-1} \cdot 10^{-9}$ cells	$zmol \cdot s^{-1} \cdot cell^{-1}$	3
Cell number concentration, C_{Nce}	10^6 cells$\cdot mL^{-1}$	10^9 cells$\cdot L^{-1}$	
Mitochondrial protein concentration, C_{mte}	0.1 mg$\cdot mL^{-1}$	0.1 g$\cdot L^{-1}$	
Mass-specific flux, $J_{m,O2}$	$pmol \cdot s^{-1} \cdot mg^{-1}$	$nmol \cdot s^{-1} \cdot g^{-1}$	4
Catabolic power, $P_{k,O2}$	$\mu W \cdot 10^{-6}$ cells	$pW \cdot cell^{-1}$	1
Volume	$1,000$ L	m^3 ($1,000$ kg)	
	L	dm^3 (kg)	
	mL	cm^3 (g)	
	μL	mm^3 (mg)	
	fL	μm^3 (pg)	
Amount of substance concentration	M = $mol \cdot L^{-1}$	$mol \cdot dm^{-3}$	

1178
1179 1 pmol: picomole = 10^{-12} mol
1180 2 amol: attomole = 10^{-18} mol
1181 3 zmol: zeptomole = 10^{-21} mol
1182 4 nmol: nanomole = 10^{-9} mol
1183

1184 *4.4. Conversion: oxygen, proton and ATP flux*

1185 $J_{O2,k}$ is coupled in mitochondrial steady states to proton cycling, $J_{\infty H+} = J_{H+,out} = J_{H+,in}$ (**Fig.**

1186 **2**). $J_{H+,out/n}$ and $J_{H+,in/n}$ [$nmol \cdot s^{-1} \cdot L^{-1}$] are converted into electrical units, $J_{H+,out/e}$

1187 [$mC \cdot s^{-1} \cdot L^{-1} = mA \cdot L^{-1}$] = $J_{H+,out/n}$ [$nmol \cdot s^{-1} \cdot L^{-1}$]$\cdot F$ [$C \cdot mol^{-1}$]$\cdot 10^{-6}$ (**Table 4**). At a $J_{H+,out}/J_{O2,k}$ ratio

1188 or H^+_{out}/O_2 of 20 ($H^+_{out}/O=10$), a volume-specific O_2 flux of 100 $nmol \cdot s^{-1} \cdot L^{-1}$ would correspond

1189 to a proton flux of 2,000 nmol $H^+_{out} \cdot s^{-1} \cdot L^{-1}$ or volume-specific current of 193 $mA \cdot L^{-1}$.

1190 $$J_{V,H+out/e}\ [mA \cdot L^{-1}] = J_{V,H+out/n} \cdot F \cdot 10^{-6}\ [nmol \cdot s^{-1} \cdot L^{-1} \cdot mC \cdot nmol^{-1}] \qquad \text{(Eq. 3.1)}$$

1191 $$J_{V,H+out/e}\ [mA \cdot L^{-1}] = J_{V,O2} \cdot (H^+_{out}/O_2) \cdot F \cdot 10^{-6}\ [mC \cdot s^{-1} \cdot L^{-1} = mA \cdot L^{-1}] \qquad \text{(Eq. 3.2)}$$

1192 ETS capacity in various human cell types including HEK 293, primary HUVEC and fibroblasts

1193 ranges from 50 to 180 $amol \cdot s^{-1} \cdot cell^{-1}$, measured in intact cells in the noncoupled state (see

1194   Gnaiger 2014). At 100 amol·s^{-1}·cell^{-1} corrected for ROX (corresponding to a catabolic power

1195   of -48 pW·cell^{-1}), the current across the mt-membranes, I_e, approximates 193 pA·cell^{-1} or 0.2

1196   nA per cell. See Rich (2003) for an extension of quantitative bioenergetics from the molecular

1197   to the human scale, with a transmembrane proton flux equivalent to 520 A in an adult at a

1198   catabolic power of -110 W. Modelling approaches illustrate the link between proton motive

1199   force and currents (Willis *et al.* 2016).For NADH- and succinate-linked respiration, the

1200   mechanistic P»/O$_2$ ratio (referring to the full 4 electron reduction of O$_2$) is calculated at 20/3.7

1201   and 12/3.7, respectively (Eq. 4) equal to 5.4 and 3.3. The classical P»/O ratios (referring to the

1202   2 electron reduction of 0.5 O$_2$) are 2.7 and 1.6 (Watt *et al.* 2010), in direct agreement with the

1203   measured P»/O ratio for succinate of 1.58 ± 0.02 (Gnaiger *et al.* 2000; for detailed reviews see

1204   Wikström and Hummer 2012; Sazanov 2015),

1205 $$P»/O_2 = (H^+_{out}/O_2)/(H^+_{in}/P») \qquad \text{(Eq. 4)}$$

1206   In summary (**Fig. 1**),

1207 $$J_{V,P»} \text{ [nmol·s}^{-1}\text{·L}^{-1}\text{]} = J_{V,O2}·(H^+_{out}/O_2)/(H^+_{in}/P») \qquad \text{(Eq. 5.1)}$$

1208 $$J_{V,P»} \text{ [nmol·s}^{-1}\text{·L}^{-1}\text{]} = J_{V,O2}·(P»/O_2) \qquad \text{(Eq. 5.2)}$$

1209   We consider isolated mitochondria as powerhouses and proton pumps as molecular machines

1210   to relate experimental results to energy metabolism of the intact cell. The cellular P»/O$_2$ based

1211   on oxidation of glycogen is increased by the glycolytic (fermentative) substrate-level

1212   phosphorylation of 3 P»/Glyc, *i.e.*, 0.5 mol P» for each mol O$_2$ consumed in the complete

1213   oxidation of a mol glycosyl unit (Glyc). Adding 0.5 to the mitochondrial P»/O$_2$ ratio of 5.4

1214   yields a bioenergetic cell physiological P»/O$_2$ ratio close to 6. Two NADH equivalents are

1215   formed during glycolysis and transported from the cytosol into the mitochondrial matrix, either

1216   by the malate-aspartate shuttle or by the glycerophosphate shuttle resulting in different

1217   theoretical yield of ATP generated by mitochondria, the energetic cost of which potentially

1218   must be taken into account. Considering also substrate-level phosphorylation in the TCA cycle,

1219   this high P»/O$_2$ ratio not only reflects proton translocation and OXPHOS studied in isolation,

1220   but integrates mitochondrial physiology with energy transformation in the living cell (Gnaiger

1221   1993a).

1222

1223   **5. Conclusions**

1224   MitoEAGLE can serve as a gateway to better diagnose mitochondrial respiratory defects

1225   linked to genetic variation, age-related health risks, sex-specific mitochondrial performance,

1226   lifestyle with its effects on degenerative diseases, and thermal and chemical environment. The

1227   present recommendations on coupling control states and rates, linked to the concept of the

1228   protonmotive force (Part 1) will be extended in a series of reports on pathway control of

1229   mitochondrial respiration, respiratory states in intact cells, and harmonization of experimental

1230   procedures.

1231

1232   **Box 5: Mitochondrial and cell respiration**

1233   Mitochondrial and cell respiration is the process of highly exothermic energy transformation in

1234   which scalar redox reactions are coupled to vectorial ion translocation across a semipermeable

1235   membrane, which separates the small volume of a bacterial cell or mitochondrion from the

1236   larger volume of its surroundings. The electrochemical exergy can be partially conserved in the

1237   phosphorylation of ADP to ATP or in ion pumping, or dissipated in an electrochemical short-

1238   circuit. Respiration is thus clearly distinguished from fermentation as the counterpart of cellular

1239   core energy metabolism. Respiration is separated in mitochondrial preparations from the partial

1240   contribution of fermentative pathways of the intact cell. According to this definition, residual

1241   oxygen consumption, as measured after inhibition of the mitochondrial electron transfer system,

1242   does not belong to the class of catabolic reactions and is, therefore, subtracted from total oxygen

1243   consumption to obtain baseline-corrected respiration.

1244

1245   The optimal choice for expressing mitochondrial and cell respiration (**Box 5**) as O_2 flow

1246   per biological system, and normalization for specific tissue-markers (volume, mass, protein)

1247   and mitochondrial markers (volume, protein, content, mtDNA, activity of marker enzymes,

1248   respiratory reference state) is guided by the scientific question. Interpretation of the obtained

1249   data depends critically on appropriate normalization, and therefore reporting rates merely as

1250 $nmol \cdot s^{-1}$ is discouraged, since it restricts the analysis to intra-experimental comparison of

1251   relative (qualitative) differences. Expressing O_2 consumption per cell may not be possible when

1252   dealing with tissues. For studies with mitochondrial preparations, we recommend that

1253   normalizations be provided as far as possible: (*1*) on a per cell basis as O_2 flow (a biophysical

1254   normalization); (*2*) per g cell or tissue protein, or per cell or tissue mass as mass-specific O_2

1255   flux (a cellular normalization); and (*3*) per mitochondrial marker as mt-specific flux (a

1256   mitochondrial normalization). With information on cell size and the use of multiple

1257   normalizations, maximum potential information is available (Renner *et al.* 2003; Wagner *et al.*

1258   2011; Gnaiger 2014). When using isolated mitochondria, mitochondrial protein is a frequently

1259   applied mitochondrial marker, the use of which is basically restricted to isolated mitochondria.

1260   Mitochondrial markers, such as citrate synthase activity as an enzymatic matrix marker, provide

1261   a link to the tissue of origin on the basis of calculating the mitochondrial yield, *i.e.*, the fraction

1262   of mitochondrial marker obtained from a unit mass of tissue.

1263

1267   **Competing financial interests:** E.G. is founder and CEO of Oroboros Instruments, Innsbruck,

1268   Austria.

1269

1270

6. References (*incomplete; www links will be deleted in the final version*)

Altmann R. Die Elementarorganismen und ihre Beziehungen zu den Zellen. Zweite vermehrte
Auflage. Verlag Von Veit & Comp, Leipzig 1894;160 pp. -
www.mitoeagle.org/index.php/Altmann_1894_Verlag_Von_Veit_%26_Comp

Birkedal R, Laasmaa M, Vendelin M. The location of energetic compartments affects
energetic communication in cardiomyocytes. Front Physiol 2014;5:376. doi:
10.3389/fphys.2014.00376. eCollection 2014. PMID: 25324784

Brown GC. Control of respiration and ATP synthesis in mammalian mitochondria and cells.
Biochem J 1992;284:1-13. - www.mitoeagle.org/index.php/Brown_1992_Biochem_J

Chance B, Williams GR. Respiratory enzymes in oxidative phosphorylation: III. The steady
state. J Biol Chem 1955;217:409-27. -
www.mitoeagle.org/index.php/Chance_1955_J_Biol_Chem-III

Chance B, Williams GR. Respiratory enzymes in oxidative phosphorylation. IV. The
respiratory chain. J Biol Chem 1955;217:429-38. -
www.mitoeagle.org/index.php/Chance_1955_J_Biol_Chem-IV

Chance B, Williams GR. The respiratory chain and oxidative phosphorylation. Adv Enzymol
Relat Subj Biochem 1956;17:65-134. -
www.mitoeagle.org/index.php/Chance_1956_Adv_Enzymol_Relat_Subj_Biochem

Cohen ER, Cvitas T, Frey JG, Holmström B, Kuchitsu K, Marquardt R, Mills I, Pavese F,
Quack M, Stohner J, Strauss HL, Takami M, Thor HL. Quantities, units and smbols in
physical chemistry, IUPAC Green Book 2008;3rd Edition, 2nd Printing, IUPAC & RSC
Publishing, Cambridge. -
www.mitoeagle.org/index.php/Cohen_2008_IUPAC_Green_Book

Coopersmith J. Energy, the subtle concept. The discovery of Feynman's blocks from Leibnitz
to Einstein. Oxford University Press 2010;400 pp.

1296   Dai Q, Shah AA, Garde RV, Yonish BA, Zhang L, Medvitz NA, Miller SE, Hansen EL, Dunn

1297   CN, Price TM. A truncated progesterone receptor (PR-M) localizes to the

1298   mitochondrion and controls cellular respiration. ???

1299   Dufour S, Rousse N, Canioni P, Diolez P. Top-down control analysis of temperature effect on

1300   oxidative phosphorylation. Biochem J 1996;314:743-51.

1301   Ernster L, Schatz G Mitochondria: a historical review. J Cell Biol 1981;91:227s-55s. -

1302   www.mitoeagle.org/index.php/Ernster_1981_J_Cell_Biol

1303   Estabrook RW. Mitochondrial respiratory control and the polarographic measurement of

1304   ADP:O ratios. Methods Enzymol 1967;10:41-7. -

1305   www.mitoeagle.org/index.php/Estabrook_1967_Methods_Enzymol

1306   Fell D. Understanding the control of metabolism. Portland Press 1997.

1307   Garlid KD, Semrad C, Zinchenko V. Does redox slip contribute significantly to mitochondrial

1308   respiration? In: Schuster S, Rigoulet M, Ouhabi R, Mazat J-P (eds) Modern trends in

1309   biothermokinetics. Plenum Press, New York, London 1993;287-93.

1310   Gerö D, Szabo C. Glucocorticoids suppress mitochondrial oxidant production via

1311   upregulation of uncoupling protein 2 in hyperglycemic endothelial cells. PLoS One

1312   2016;11:e0154813.

1313   Gnaiger E. Efficiency and power strategies under hypoxia. Is low efficiency at high glycolytic

1314   ATP production a paradox? In: Surviving Hypoxia: Mechanisms of Control and

1315   Adaptation. Hochachka PW, Lutz PL, Sick T, Rosenthal M, Van den Thillart G (eds.)

1316   CRC Press, Boca Raton, Ann Arbor, London, Tokyo 1993a:77-109. -

1317   www.mitoeagle.org/index.php/Gnaiger_1993_Hypoxia

1318   Gnaiger E. Nonequilibrium thermodynamics of energy transformations. Pure Appl Chem

1319   1993b;65:1983-2002. - www.mitoeagle.org/index.php/Gnaiger_1993_Pure_Appl_Chem

1320   Gnaiger E. Bioenergetics at low oxygen: dependence of respiration and phosphorylation on

1321   oxygen and adenosine diphosphate supply. Respir Physiol 2001;128:277-97. -

1322   www.mitoeagle.org/index.php/Gnaiger_2001_Respir_Physiol

1323   Gnaiger E. Mitochondrial pathways and respiratory control. An introduction to OXPHOS

1324   analysis. 4th ed. Mitochondr Physiol Network 2014;19.12. Oroboros MiPNet

1325   Publications, Innsbruck:80 pp. -

1326   www.mitoeagle.org/index.php/Gnaiger_2014_MitoPathways

1327   Gnaiger E. Capacity of oxidative phosphorylation in human skeletal muscle. New

1328   perspectives of mitochondrial physiology. Int J Biochem Cell Biol 2009;41:1837-45. -

1329   www.mitoeagle.org/index.php/Gnaiger_2009_Int_J_Biochem_Cell_Biol

1330   Gnaiger E, Méndez G, Hand SC. High phosphorylation efficiency and depression of

1331   uncoupled respiration in mitochondria under hypoxia. Proc Natl Acad Sci USA

1332   2000;97:11080-5. -

1333   www.mitoeagle.org/index.php/Gnaiger_2000_Proc_Natl_Acad_Sci_U_S_A

1334   Hofstadter DR. Gödel, Escher, Bach: An eternal golden braid. A metaphorical fugue on minds

1335   and machines in the spirit of Lewis Carroll. Harvester Press 1979;499 pp. -

1336   www.mitoeagle.org/index.php/Hofstadter_1979_Harvester_Press

1337   Illaste A, Laasmaa M, Peterson P, Vendelin M. Analysis of molecular movement reveals

1338   latticelike obstructions to diffusion in heart muscle cells. Biophys J 2012;102:739-48. -

1339   PMID: 22385844

1340   Jepihhina N, Beraud N, Sepp M, Birkedal R, Vendelin M. Permeabilized rat cardiomyocyte

1341   response demonstrates intracellular origin of diffusion obstacles. Biophys J

1342   2011;101:2112-21. - PMID: 22067148

1343   Komlódi T, Tretter L. Methylene blue stimulates substrate-level phosphorylation catalysed by

1344   succinyl-CoA ligase in the citric acid cycle. Neuropharmacology 2017;123:287-98. -

1345   www.mitoeagle.org/index.php/Komlodi_2017_Neuropharmacology

1346   Lee SR, Kim HK, Song IS, Youm J, Dizon LA, Jeong SH, Ko TH, Heo HJ, Ko KS, Rhee BD,

1347   Kim N, Han J. Glucocorticoids and their receptors: insights into specific roles in

1348   mitochondria. Prog Biophys Mol Biol 2013;112:44-54.

1349   Lemieux H, Blier PU, Gnaiger E. Remodeling pathway control of mitochondrial respiratory

1350   capacity by temperature in mouse heart: electron flow through the Q-junction in

1351   permeabilized fibers. Sci Rep 2017;7:2840. -

1352   www.mitoeagle.org/index.php/Lemieux_2017_Sci_Rep

1353   Lenaz G, Tioli G, Falasca AI, Genova ML. Respiratory supercomplexes in mitochondria. In:

1354   Mechanisms of primary energy trasduction in biology. M Wikstrom (ed) Royal Society

1355   of Chemistry Publishing, London, UK 2017:296-337 (in press)

1356   Margulis L. Origin of eukaryotic cells. New Haven: Yale University Press 1970.

1357   Meinild Lundby AK, Jacobs RA, Gehrig S, de Leur J, Hauser M, Bonne TC, Flück D,

1358   Dandanell S, Kirk N, Kaech A, Ziegler U, Larsen S, Lundby C. Exercise training

1359   increases skeletal muscle mitochondrial volume density by enlargement of existing

1360   mitochondria and not de novo biogenesis. Acta Physiol (Oxf) 2017;[Epub ahead of

1361   print].

1362   Miller GA. The science of words. Scientific American Library New York 1991;276 pp. -

1363   www.mitoeagle.org/index.php/Miller_1991_Scientific_American_Library

1364   Mitchell P. Chemiosmotic coupling in oxidative and photosynthetic phosphorylation Biochim

1365   Biophys Acta Bioenergetics 2011;1807:1507-38. -

1366   http://www.sciencedirect.com/science/article/pii/S0005272811002283

1367   Mitchell P, Moyle J. Respiration-driven proton translocation in rat liver mitochondria.

1368   Biochem J 1967;105:1147-62. -

1369   www.mitoeagle.org/index.php/Mitchell_1967_Biochem_J

1370   Moreno M, Giacco A, Di Munno C, Goglia F. Direct and rapid effects of 3,5-diiodo-L-

1371   thyronine (T2). Mol Cell Endocrinol 2017;7207:30092-8.

1372 Morrow RM, Picard M, Derbeneva O, Leipzig J, McManus MJ, Gouspillou G, Barbat-Artigas

1373   S, Dos Santos C, Hepple RT, Murdock DG, Wallace DC. Mitochondrial energy

1374   deficiency leads to hyperproliferation of skeletal muscle mitochondria and enhanced

1375   insulin sensitivity. Proc Natl Acad Sci U S A 2017;114:2705-10. -

1376   www.mitoeagle.org/index.php/Morrow_2017_Proc_Natl_Acad_Sci_U_S_A

1377 Nicholls DG, Ferguson S. Bioenergetics 4. Elsevier 2013.

1378 Paradies G, Paradies V, De Benedictis V, Ruggiero FM, Petrosillo G. Functional role of

1379   cardiolipin in mitochondrial bioenergetics. Biochim Biophys Acta 2014;1837:408-17. -

1380   http://www.mitoeagle.org/index.php/Paradies_2014_Biochim_Biophys_Acta

1381 Price TM, Dai Q. The Role of a Mitochondrial Progesterone Receptor (PR-M) in

1382   Progesterone Action. Semin Reprod Med. 2015;33:185-94.

1383 Prigogine I. Introduction to thermodynamics of irreversible processes. Interscience, New

1384   York, 1967;3rd ed.

1385 Puchowicz MA, Varnes ME, Cohen BH, Friedman NR, Kerr DS, Hoppel CL. Oxidative

1386   phosphorylation analysis: assessing the integrated functional activity of human skeletal

1387   muscle mitochondria – case studies. Mitochondrion 2004;4:377-85. -

1388   www.mitoeagle.org/index.php/Puchowicz_2004_Mitochondrion

1389 P. M. Quiros, A. Mottis, and J. Auwerx. Mitonuclear communication in homeostasis and

1390   stress. Nat Rev Mol Cell Biol 2016;17:213-26.

1391 Renner K, Amberger A, Konwalinka G, Gnaiger E. Changes of mitochondrial respiration,

1392   mitochondrial content and cell size after induction of apoptosis in leukemia cells.

1393   Biochim Biophys Acta 2003;1642:115-23. -

1394   www.mitoeagle.org/index.php/Renner_2003_Biochim_Biophys_Acta

1395 Rich P. Chemiosmotic coupling: The cost of living. Nature 2003;421:583. -

1396   www.mitoeagle.org/index.php/Rich_2003_Nature

1397 Rostovtseva TK, Sheldon KL, Hassanzadeh E, Monge C, Saks V, Bezrukov SM, Sackett DL.

1398 Tubulin binding blocks mitochondrial voltage-dependent anion channel and regulates

1399 respiration. Proc Natl Acad Sci USA 2008;105:18746-51. -

1400 www.mitoeagle.org/index.php/Rostovtseva_2008_Proc_Natl_Acad_Sci_U_S_A

1401 Rustin P, Parfait B, Chretien D, Bourgeron T, Djouadi F, Bastin J, Rötig A, Munnich A.

1402 Fluxes of nicotinamide adenine dinucleotides through mitochondrial membranes in

1403 human cultured cells. J Biol Chem 1996;271:14785-90.

1404 Saks VA, Veksler VI, Kuznetsov AV, Kay L, Sikk P, Tiivel T, Tranqui L, Olivares J, Winkler

1405 K, Wiedemann F, Kunz WS. Permeabilised cell and skinned fiber techniques in studies

1406 of mitochondrial function in vivo. Mol Cell Biochem 1998;184:81-100. -

1407 http://www.mitoeagle.org/index.php/Saks_1998_Mol_Cell_Biochem

1408 Salabei JK, Gibb AA, Hill BG. Comprehensive measurement of respiratory activity in

1409 permeabilized cells using extracellular flux analysis. Nat Protoc 2014;9:421-38.

1410 Sazanov LA. A giant molecular proton pump: structure and mechanism of respiratory

1411 complex I. Nat Rev Mol Cell Biol 2015;16:375-88. -

1412 www.mitoeagle.org/index.php/Sazanov_2015_Nat_Rev_Mol_Cell_Biol

1413 Schönfeld P, Dymkowska D, Wojtczak L. Acyl-CoA-induced generation of reactive oxygen

1414 species in mitochondrial preparations is due to the presence of peroxisomes. Free Radic

1415 Biol Med 2009;47:503-9.

1416 Schrödinger E. What is life? The physical aspect of the living cell. Cambridge Univ Press,

1417 1944. - www.mitoeagle.org/index.php/Gnaiger_1994_BTK

1418 Simson P, Jepihhina N, Laasmaa M, Peterson P, Birkedal R, Vendelin M. Restricted ADP

1419 movement in cardiomyocytes: Cytosolic diffusion obstacles are complemented with a

1420 small number of open mitochondrial voltage-dependent anion channels. J Mol Cell

1421 Cardiol 2016;97:197-203. - PMID: 27261153

1422 Stucki JW, Ineichen EA. Energy dissipation by calcium recycling and the efficiency of

1423   calcium transport in rat-liver mitochondria. Eur J Biochem 1974;48:365-75.

1424 Wagner BA, Venkataraman S, Buettner GR. The rate of oxygen utilization by cells. Free

1425   Radic Biol Med. 2011:51:700-712.

1426   http://dx.doi.org/10.1016/j.freeradbiomed.2011.05.024 PMCID: PMC3147247

1427 Watt IN, Montgomery MG, Runswick MJ, Leslie AG, Walker JE. Bioenergetic cost of

1428   making an adenosine triphosphate molecule in animal mitochondria. Proc Natl Acad Sci

1429   U S A 2010;107:16823-7. -

1430   www.mitoeagle.org/index.php/Watt_2010_Proc_Natl_Acad_Sci_U_S_A

1431 Weibel ER, Hoppeler H. Exercise-induced maximal metabolic rate scales with muscle aerobic

1432   capacity. J Exp Biol 2005;208:1635–44.

1433 Wikström M, Hummer G. Stoichiometry of proton translocation by respiratory complex I and

1434   its mechanistic implications. Proc Natl Acad Sci U S A 2012;109:4431-6. -

1435   www.mitoeagle.org/index.php/Wikstroem_2012_Proc_Natl_Acad_Sci_U_S_A

1436 Willis WT, Jackman MR, Messer JI, Kuzmiak-Glancy S, Glancy B. A simple hydraulic

1437   analog model of oxidative phosphorylation. Med Sci Sports Exerc. 2016;48:990-1000.